Towards a UV model of kinetic mixing and portal matter

Thomas D. Rueter[1,2,*] and Thomas G. Rizzo[2,†]
[1]*Stanford University, Stanford, California 94305, USA*
[2]*SLAC National Accelerator Laboratory, Stanford University, Menlo Park, California 94025, USA*

(Received 7 October 2019; published 24 January 2020)

The nature of dark matter (DM) and how it might interact with the particles of the Standard Model (SM) is an ever-growing mystery. It is possible that the existence of new "dark sector" forces, yet undiscovered, are the key to solving this fundamental problem, and one might hope that in the future such forces might even be "unified" with the ones we already know in some UV-complete framework. In this paper, following a bottom-up approach, we attempt to take the first steps in the construction of such a framework. The much-discussed possibility of the kinetic mixing (KM) of the "dark photon" with the hypercharge gauge boson of the SM via loops of portal matter (PM) fields, charged in both sectors, offers an attractive starting point for these efforts. Given the anticipated finite strength of the KM in a UV-complete theory, the absence of anomalies, and the lifetime constraints on the PM fields arising from cosmic microwave background and nucleosynthesis constraints, PM must behave as vector-like copies of the known SM fermion fields, such as those which appear naturally in, e.g., E_6-type models. Within such a setup, the SM and their corresponding partner PM fields would be related by a new $SU(2)_I$ gauge symmetry. With this observation as a springboard, we construct a generalization of these ideas where $SU(2)_I$ is augmented by an additional $U(1)_{I_Y}$ factor so that the light dark photon is the result of a symmetry breaking analogous to the SM, i.e., $SU(2)_I \times U(1)_{I_Y} \to U(1)_D$, but with $U(1)_D$ now also broken at the $\lesssim$GeV scale. While SM fields are $U(1)_D$ singlets, as in the conventional dark photon approach, they transform nontrivially under the full $SU(2)_I \times U(1)_{I_Y}$ gauge group. This approach leads to numerous interesting signatures, both at low energies and at colliders, and can be viewed as an initial step in the construction of a more UV-complete framework.

DOI: 10.1103/PhysRevD.101.015014

I. INTRODUCTION

The nature of dark matter (DM) is one of our biggest mysteries and points to there being new physics beyond the Standard Model (SM). Historically, the favorite candidates for DM originated in top-down theories which addressed other outstanding problems within the SM such as axions [1,2] and weakly interacting massive particles (WIMPs) [3]. While so far obtaining only null results, important experimental searches for such states are ongoing. However, these as-yet null results, in addition to the realization of how large the parameter space for potential DM candidates might be, have inspired both increased model-building activity and the ever-widening scope of experimental DM searches [4,5]. In almost all DM scenarios, new forces carried by non-SM mediator particles are needed to pass through the SM–dark sector barricade thrown down by nature and convey the interaction between the DM and the SM that is responsible for the DM obtaining its observed relic density [6]. Among these, one of the most experimentally accessible and also well-studied scenarios is that of the dark photon (DP)/vector portal model [7]. In its simplest form, one imagines a new, broken dark $U(1)_D$ gauge group associated with a massive vector dark photon, V; here we will assume this symmetry is broken by the vacuum expectation value (VEV) of a SM singlet dark Higgs field, S, at the ∼GeV scale. While DM carries a nontrivial dark charge, Q_D, it is assumed that the SM fields do not and so are not directly coupled to V. However, via the kinetic mixing (KM) [8] of V with the familiar SM $U(1)_Y$ weak hypercharge gauge boson, B, after electroweak symmetry breaking the SM fields pick up a small coupling to V proportional to their electric charge, $\epsilon e Q_{em}$. Here ϵ describes the strength of the KM [8] and thus the suppression of our interactions with the dark sector is due to the small, loop-induced value of this parameter in such a scenario. While this is an extremely interesting setup, it is likely to only be an IR shadow of a much larger

*tdr38@stanford.edu
†rizzo@slac.stanford.edu

and more complex UV-complete theory which may have implications beyond just the, now potentially more intricate, dark sector.

In our earlier work [9], hereafter designated as **I**, we took the first step on the way to the construction of a more UV-complete KM scenario; it is the purpose of this paper to take a further step in this direction. The point of view taken in **I** is that the KM-generating mechanism itself may provide the first hint to the direction we should follow. As is well known, KM is generated by the existence of sets of fields, here called portal matter (PM), that carry both dark charges as well as, at the very least, SM weak hypercharge thus linking the two $U(1)$ factors via a one-loop vacuum polarization-like diagram. In **I** we argued that in a complete UV theory the strength of KM, ϵ, is a finite, in principle calculable, quantity as it is in grand unified theories (GUTs) [10] with split multiplets. This hypothesis, when combined with the necessity that such new states be unstable since they carry SM quantum numbers, led to a number of restrictions on the nature of the possible portal matter fields. If such fields are fermionic, as posited in **I**, they must be also be vector-like [11,12] with respect to the SM to avoid both gauge anomalies and any conflict with precision electroweak measurements [13]. This led us to consider the rather unique possibility that portal matter can only transform as vector-like copies [11] of one or more of the usual SM fermion fields.[1] In **I**, in order to obtain a finite, radiatively generated ϵ, we considered toy models wherein the portal matter consisted of two vector-like copies of a single SM field with opposite dark charges thus rendering ϵ finite in a rather trivial manner. However, there we also briefly discussed the more complex, and perhaps much more interesting, possibility that portal matter may consist of a set of different vector-like fields with various SM quantum numbers whose infinite contributions to ϵ "naturally" cancel among themselves, as might be the case if they formed, e.g., a $5+\bar{5}$ of $SU(5)$, as a potential way forward in constructing more realistic UV-complete theories. This is the direction that we will follow in this paper.

An extension of the SM by an additional $5+\bar{5}$ of $SU(5)$ cannot help but remind (some of) us of grand unification based on the group E_6, where such an additional set of fields naturally occurs [15]. Such models proved of great phenomenological interest some time ago in connection with the early developments in string theory [15] in the late 1980s. In such a framework, not only was the matter sector of the SM extended but also generally present were SM gauge sector augmentations by various species of $U(1)$ and/or $SU(2)$ factors increasing the complexity of the resulting phenomenology. Of course, in the case under discussion here, the obvious gauge sector extension of interest is $U(1)_D$ for which all of the SM fields are neutral, unlike what we find in the case of new the $U(1)$'s which appear in E_6. However, also with an eye towards future work, some of the basic ideas in E_6-type setups, as we will see below, can provide a good jumping-off point for moving forward. The fact that the SM fields all have $Q_D=0$ tells us that we will actually need to go beyond the simple E_6 picture to obtain a viable model, as has been recently noted in the literature [16], and we will take a bottom-up approach in extending the E_6 setup in what follows. The general setup which we present below is, to say the least, somewhat fine-tuned; how much that should disturb us at this point is up to one's tastes. However, we should be reminded that the work here presents only a preliminary step on the way to a more UV-complete theory involving the SM, DM and the portal matter responsible for their mutual interaction, which may result in a reduction of this fine-tuning or at least make such fine-tuning more palatable.

The outline of this paper is as follows. Section II contains a general background discussion and an overview of our model setup using arguments from both top-down and bottom-up approaches. Section III provides a discussion on the various components of our setup in the gauge and fermion sectors and the relevant couplings and mixings among the physical states relevant for the discussions that follow. Section IV contains a mainly collider-oriented view of some of the physics associated with the new exotic particles we have introduced while Sec. V contains a discussion of some DM physics within the present setup. Finally, the last section summarizes our results and conclusions and points us in the direction of our next steps.

II. BACKGROUND AND MODEL SETUP

In order to attempt to construct a GUT-inspired, UV-complete theory of both the DM and PM sectors as well as their interactions with the SM it is necessary to have some preliminary target properties in mind that we would expect such a theory to possess. Similarly, we should have a parallel set of, potentially overlapping, expectations for the low(er)-energy theory operating at the $\sim$ few TeV scale and below as clearly one might also anticipate that the lower-energy theory will inherit some of the properties found in the high-scale theory. As was discussed briefly in **I** and mentioned above in the Introduction, to allow for their instability, new vector-like (with respect to the SM gauge group) candidate fermionic portal matter fields in their simplest manifestation must transform in a manner similar to that of some subset of SM fermionic representations, i.e., $SU(3)_c$ color singlets and triplets which also fall into $SU(2)_L$ weak-isospin singlets or doublets.[2] As such, these portal matter states automatically carry a set of weak

[1] We note that such PM states have gotten little attention in the literature [14].

[2] Note that this is already suggestive that a symmetry may exist relating these portal matter fields to their SM "partners."

hypercharges, Y_i, matching those of the corresponding conventional SM fermions. If these portal matter fields are assigned dark charges, $Q_{D_i} \neq 0$, then a *finite*, one-loop-induced value for the KM mixing between a light, $\lesssim$GeV, dark $U(1)_D$ gauge field and the corresponding $U(1)_Y$ hypercharge field, can be induced. As described above, and in the notation of **I**, the parameter describing this KM is essentially given by

$$\epsilon \sim \frac{g_D g_Y}{12\pi^2} \sum_i Y_i Q_{D_i} \left(\text{pole} + \ln \frac{m_i^2}{\mu^2} \right) \tag{1}$$

where $g_{D,Y}$ are the $U(1)_{D,Y}$ gauge couplings and "pole" is the usual singular plus mass-independent constant piece obtained in dimensional regularization. ϵ will be generated via the various contributing particle mass differences and will also prove to be *finite* and μ-independent provided that the condition $\sum_i Y_i Q_{D_i} = 0$ is satisfied. From a purely low-energy perspective, this requirement would appear to be *ad hoc* but should be expected to be a natural property of the UV theory as was speculated in **I**. As is well known, in a GUT-like framework, for any given representation, $\mathrm{Tr} T_i T_j = 0\,(i \neq j)$ is found to hold automatically for any two distinct generators, T_i, which in the case at hand renders the KM parameter ϵ finite and calculable in such models [10] if both Y and Q_D correspond to (linear combinations of distinct) generators of the UV gauge group. This calculability of the analogs of ϵ in GUT theories with split representations was already made use of long ago [10] for model-building/phenomenological purposes.

To gain some further insight into these issues and to provide a point of departure for the analysis that follows, let us briefly consider the anomaly-free GUT group E_6 [15] whose fundamental representation, 27, contains the usual 15 SM chiral fermions together with 12 additional "exotic," (almost) vector-like fermions (VLFs). Of particular interest to us here is the decomposition of E_6 into one of its maximal subgroups $SU(2)_I \times SU(6)$ [17] under which the fundamental 27 representation decomposes as $27 \to (2, \bar{6}) + (1, 15)$, where the first [second] number is the dimension of the corresponding $SU(2)_I$ [$SU(6)$] representation. This $SU(2)_I$ gauge group will play an important role in our discussion below. When the $SU(6)$ group then breaks to the familiar $SU(5) \times U(1)_6$, where $SU(5)$ will be used here in the following discussion as just a proxy for the SM, one then has $27 \to (2, \bar{5})_{-1} + (2, 1)_5 + (1, 5)_{-4} + (1, 10)_2$ where the second number now labels the $SU(5)$ representation and the numbers written as subscripts are the corresponding $U(1)_6$ charges. Here we see the well-known result that the new exotic fermions lie in a pair of $SU(5)$ $5 + \bar{5}$ representations as well as a pair of $SU(5)$ singlets. Following Ref. [15] we will denote the vector (left-handed) fields in the $\bar{5}$ as $(N, E)_L^T$, h_L^c, with the corresponding conjugate fields in the 5. While h_L^c is a color (anti)triplet, weak isosinglet, transforming similarly to $\sim d_L^c$, $(N, E)_L^T$ is a color singlet, weak isodoublet, transforming similarly to $\sim(\nu, e)_L^T$, and together with the content of the 5 these fields form a set of fermions which are vector-like with respect to the SM. The additional SM singlets in the $(2, 1)_5$ are usually suggestively denoted as ν^c and S^c [15] but here we simply refer to them as $S_{1,2}$. Why is this E_6 structure interesting from the portal matter perspective? Here we have an anomaly-free setup which already contains vector-like fermions which transform under the SM in a manner analogous to (some of) the SM fermions thus being able to play the role of portal matter and which are related to the SM by the action of the $SU(2)_I$ group, i.e., the value of T_{3I} differentiates the SM from exotic fields. Such a possibility was already foreseen in **I**. Furthermore, if we were to (mistakenly as we will soon see) identify Q_D with this diagonal generator then the above requirement, the condition $TrYQ_D = 0$ would be automatically satisfied so that ϵ would indeed be finite and calculable at one loop as desired. One could go even further and imagine that at some large scale, say $\sim$10 TeV, the breaking $SU(2)_I \to U(1)_D$ via a real $SU(2)_I$ triplet would give heavy masses to the non-Hermitian "off-diagonal" $W_I^{(\dagger)}$ gauge bosons coupling to the non-Hermitian pair of $SU(2)_I$ isospin-raising and -lowering operators and thus identify the diagonally coupled W_I^0 with the dark photon which is left to get mass at the $\sim$GeV scale or below. Assuming that the $SU(2)_I$ gauge coupling, g_I, is even remotely close in magnitude to the usual weak coupling this seemingly successful and interesting approach hits a significant snag, i.e., in such a setup the dark photon will have significant couplings, $\sim g_I T_{3I}$, to some of the SM fields (since they carry $T_{3I} \neq 0$) beyond those usually induced by the loop-suppressed KM. This is inconsistent with the desired properties of the dark photon outlined above; thus, we see that we cannot make the identification of Q_D with T_{3I}, and that the dark photon cannot be embedded in this simple E_6-inspired framework. This setup does have a number of very nice features, but some important ingredients are still missing. To keep these nice features while repairing the problems we need to go beyond the simple E_6 framework.

First, let us establish some simplifying notation: we will denote the SM $SU(3)_c \times SU(2)_L \times U(1)_Y$ group structure as $3_c 2_L 1_Y$. Similarly, the above E_6 decomposition would then be written as $E_6 \to 2_I 6 \to 2_I 5 1_6$ and the relevant gauge group above the $\sim$10 TeV scale described above then would be $3_c 2_L 1_Y 2_I$, since $SU(5)$ is broken at the very high mass scale $\gtrsim 10^{14-16}$ GeV. Next, we will take a bottom-up approach to discover what it is we need to add to the previous E_6-inspired setup to maintain the attractive features above while avoiding the dark photon coupling problem. For the moment, we keep the fermionic matter content of the model the same as that in the previous paragraph. Let us imagine that we augment the 2_I gauge

group by an additional $U(1)_{I'} = U(1)_{I_Y}$ (which we will use interchangeably below) with its own gauge coupling $g_I'(= g_{I_Y})$ so that above ~10 TeV the relevant group is now $3_c 2_L 1_Y 2_I 1_{I_Y}$. In such an approach, the relevant KM is then between the usual SM hypercharge gauge boson and the corresponding gauge boson of 1_{I_Y} so that, e.g., $\epsilon \sim \sum_i Y_i Y_{I_i} \ln(m_i^2/\mu^2)$. In a sense the SM electroweak group is now seen to be "mirrored" in "I space," but with several important differences. We now further imagine that at the ~10 TeV breaking scale $2_I 1_{I_Y} \to 1_D$, i.e., $U(1)_D$ with a (at this scale) massless dark photon via a 2_I doublet VEV (which we will call v_I for the moment), in a manner completely analogous to the Higgs in the SM. This is now very familiar physics: to first approximation the W_I gets a mass $\simeq g_I v_I/2$ while the Z_I, which couples to a linear combination of the T_{3I} and Y_I generators, gets a mass $\simeq \sqrt{g_I^2 + g_I'^2} v_I/2$ so that $M_{Z_I} = M_{W_I}/c_I$, etc. (where $c_I = \cos\theta_I$ with $\tan\theta_I = g_{I_Y}/g_I$, again in complete analogy with the SM). Similarly, the dark photon, which couples to the combination $Q_I = T_{3I} + Y_I/2$, remains massless down to the ~1 GeV scale where $U(1)_D$, literally dark QED, is broken. Note that quite generally the couplings of the Z_I to the additional E_6 matter fields will now be quite different than in the E_6 case itself due to the additional $U(1)_{I_Y}$ factor. Furthermore, for a range of $x_I = s_I^2 > 0.75$, the Z_I can decay to $W_I W_I^\dagger$, which is kinematically forbidden in the ordinary E_6-inspired setup.

The low-energy theory, at/below ~10 TeV, in now seen to have three relevant, but widely separated, scales: ~10 TeV where a VEV $\sim v_I$ breaks $2_I 1_{I_Y} \to 1_D$, the usual ~250 GeV electroweak scale where $2_L 1_Y \to 1_{\rm QED}$ and the ~GeV scale where 1_D is broken and the dark photon obtains a mass. We now ask: in such a setup is it possible to assign the Y_I charges consistently to the various $3_c 2_L 1_Y 2_I 1_{I_Y}$ matter representations so that $Q_I = 0$ holds for all SM fields while the exotic fermions carry $Q_I \neq 0$, thus allowing us to identify Q_I with Q_D? As we will shortly see the answer to this question is in the affirmative.

Since, as we will see, all of the fermions in the 27 of E_6 which transform nontrivially under 2_I must also have 1_{I_Y} charges, while the SM fermions which are singlets under 2_I must not receive 1_{I_Y} charges to avoid coupling to the dark photon, it is immediately clear that we cannot identify 1_{I_Y} with the 1_6 arising from the E_6 breaking above. This implies that 1_{I_Y} is *not* a subgroup of E_6, and furthermore that the relevant GUT-like group is not the direct product $E_6 \times 1_{I_Y}$, as this would cause all fields in the 27 to have the same charge under 1_{I_Y}.[3] Hence, at higher scales $3_c 2_L 1_Y 2_I 1_{I_Y}$ (or more compactly $2_I 1_{I_Y} 5$) must be part of a larger group, e.g., $SU(8)$, which does not contain E_6 as a subgroup. Thus, while E_6 has and will continue to inspire and provide us some guidance in our model construction, especially in the matter sector, it will not directly feature in the final UV aspects of the present work. In later work [18] we will more explicitly discuss how the present framework fits into a more unified GUT-like structure.

III. REALIZING THE BOTTOM-UP MODEL

A. Basic model structure

Although we will not make explicit use of the E_6 group below, comparisons with that quite familiar scenario which leads to the additional $SU(2)_I$ gauge group with the specific model we consider here will often prove useful. At the most basic level of $3_c 2_L 1_Y 2_I 1_{I'}$, the fermion fields as described above will fall into a number of distinct representations. Here, where relevant, we assign the (conjugate) SM fields to be the $T_{3I} = 1/2(-1/2)$ "upper (lower) member" of 2_I left-handed doublets with the corresponding exotic (conjugate) fields then having $T_{3I} = -1/2(1/2)$. The fields in the familiar $SU(5)$ 10 representation —$(u,d)_L^T$, u_L^c, and e_L^c—are thus singlets under $2_I 1_{I'}$ in analogy with the case describe above, i.e., $(u,d)_L^T \sim (3,2,1/6,1,0)$, $u_L^c \sim (\bar{3},1,2/3,1,0)$ and $e_L^c \sim (1,1,1,1,0)$ under $3_c 2_L 1_Y 2_I 1_{I'}$, respectively.[4] On the other hand, all the other exotic fields (and the remaining SM ones) are then found to transform nontrivially, e.g., $(E^c, N^c)_L^T \sim (1,2,1/2,1,1)$ and $h_L \sim (3,1,-1/3,1,1)$. The remaining leptonic fields are then seen to form a bidoublet under $2_L 2_I$ similar to what one encounters in the left-right symmetric model [19], $[(\nu,e)^T;(N,E)^T]_L \sim (1,2,-1/2,2,-1/2)$ with the 2_L (2_I) generators acting vertically (horizontally) while $(h^c, d^c)_L$ is a 2_L singlet but a 2_I doublet $\sim(\bar{3},1,1/3,2,-1/2)$. Finally, we also have the SM singlets $(S_2, S_1)_L \sim (1,1,0,2,-1/2)$; as a further distinction from the pure E_6 model we will now make this representation also vector-like under 2_I by adding the corresponding conjugate fields, $(S_1^c, S_2^c)_L \sim (1,1,0,2,1/2)$, to the spectrum which will assist in our model-building efforts below. Note that this is a particular convenient *choice* and alternatives are possible where these fields remain two-component fields which obtain a Majorana mass. A short calculation shows that indeed the fermionic contributions to $TrYY_I = 0$ so that ϵ is in fact finite and calculable in this setup (assuming a similar cancellation happens in the scalar sector). It is also important to note that the above assignments lead to $Q_I = T_{3I} + Y_I/2 = 0$ for all SM fields (and also S_2) while their exotic partners have $Q_I(h_{L,R}) = 1$ and $Q_I(N,E,S_1)_{L,R} = -1$ so that the dark photon, $V = A_I$, prior to mixing does not couple to the SM but couples in a

[3]We note that the generator Y_I does *not*, in fact, commute in general with those of E_6, so this is not just $E_6 \times U(1)_{I'}$ and instead some other large unification group would be relevant at very high scales.

[4]Note that when discussing SM fermions we will employ first-generation labels.

vector-like manner to all the exotic fermions. Note further that $TrQ_I = 0$ as one might expect from any linear combination of GUT [here $SU(6)$-like] generators. In general, it may be that the exotics pair up only with one of the SM generations and not the others or that there are exotic partners for all three SM generations; we will keep these possibilities open in the discussion below but for convenience continue to employ first-generation labels, constructing the model in a single generation language.

An observation that we will *not* make use of here to keep the discussion general is that the fermion and Higgs fields that we introduce naturally fit into the embedding $2_I 1_{I'} \to 3_I$, with $SU(3)_I$ broken at an even larger mass scale. We will return to this observation in later work as it provides one of the natural next steps in the construction of a more UV-complete model.

Given the augmentation of both the low-energy ($\sim$10 TeV) gauge group and the particle content one can ask if the gauge and mixed gauge-gravity anomalies still cancel in the case of $3_c 2_L 1_Y 2_I 1_{I'}$ as they did automatically in the previously described E_6 group; the vector-like nature of much of the above structure is helpful here, but we note that fermion fields are generally *not* vector-like under $2_I 1_{I'}$ itself.[5] As might be expected, all of the dozen or so potential anomaly contributions involving only SM gauge fields or admixtures of SM gauge fields with those of $2_I 1_{I'}$ or gravity are found to cancel completely as do those arising from $SU(2)_I^3$, i.e., $TrT_{3I}^3 (= 0)$, and the mixed gauge-gravity case $TrY_I (= 0)$. However, two of the necessary anomaly-free conditions (assuming only a single generation of exotic fermions), $TrT_{3I}^2 (Y_I/2) = -5/4$ and $Tr(Y_I/2)^3 = 15/4$, are clearly nonzero so that further additional fermions must be added to the spectrum. Provided that they are SM singlets, which is certainly the simplest possibility, we need only ensure that the condition $TrY_I = 0$ remains valid when these new fermions are included. There are several possible solutions, with the simplest being the addition of a left-handed 2_I triplet, T_L, with $Y_I/2 = 1$ plus a left-handed 2_I doublet, D_L, with $Y_I/2 = -3/2$; the specific choice of such new fields will not be of direct interest in the discussion below. Of course, in a bottom-up approach we can always add further vector-like fermions as long as they do not spoil this anomaly cancellation. These fields will play very little role in the phenomenological discussions below. The fermionic content of the model discussed above, including the minimal content required for anomaly cancellation, is summarized in Table I.

In order to generate all of the gauge and fermion masses as well as the appropriate hierarchy of mass scales, $\sim$10 TeV, $\sim$250 GeV and $\sim$ at most a few GeV, several different Higgs fields are required which will transform nontrivially under the SM, $2_I 1_I$, or both. This requires a scalar sector only slightly larger than in the usual $SU(2)_I$ model with some parameter tuning necessary to generate the hierarchal VEV structure. The easiest way to uncover these Higgs fields is to require that all of the previously discussed fermions obtain masses at the appropriate scales while simultaneously maintaining the desired hierarchy of gauge symmetry breakings. This will, of course, require some fine-tuning in the Higgs potential. The simplest situation is the case of the u quark, as neither of its chiral components carries any $2_I 1_{I'}$ quantum numbers. A conventional SM-like Higgs doublet $H_1 = (H^+, H^0)^T \sim (1, 2, 1/2, 1, 0)$ can thus generate a mass term via the coupling

$$\lambda_u \bar{u}_R \begin{pmatrix} u_L \\ d_L \end{pmatrix}_i \begin{pmatrix} H^+ \\ H^0 \end{pmatrix}_j \epsilon^{ij} + \text{H.c.}, \tag{2}$$

when H^0 obtains a VEV $\langle H^0 \rangle = v/\sqrt{2}$ with $v \sim 100$ GeV. For the d quark, a different multiplet, H_2, is required, with a Yukawa coupling of the form

$$\lambda_d (\, \bar{h}_R \quad \bar{d}_R \,)_J \begin{pmatrix} u_L \\ d_L \end{pmatrix}_i \begin{pmatrix} h_1^0 & h_2^0 \\ h_1^- & h_2^- \end{pmatrix}_{jJ} \epsilon^{ij} + \text{H.c.}, \tag{3}$$

from which it is clear that H_2 is a $2_L 2_I$ bidoublet, $H_2 \sim (1, 2, -1/2, 2, 1/2)$. We have adopted the convention that $SU(2)_L$ indices i label rows while $SU(2)_I$ indices I label columns. Note that since both of the $T_{3L} = 1/2$ entries in H_2 are electrically neutral, $h_{1,2}^0$, both of these fields may obtain VEVs, $v_{1,2}/\sqrt{2}$, with $v_2 \sim 100$ GeV. Since $Q_I(h_{1,2}^0) = 1, 0$, v_2 (in combination with v above) breaks the SM gauge group but has no impact on $U(1)_D$. On the other hand, since h_1^0 carries a dark charge its VEV generates a mass for the dark photon and so $v_1 \sim$ a few GeV or less. Thus we see that while v_2 generates the d mass, $v_1 \neq 0$ generates mass mixing between d and h, a role filled by the dark Higgs in **I**. Furthermore, as we will see below, since h_1^0 has *both* T_{3L} and $Q_I \neq 0$ it also generates a mass mixing between the dark photon and the SM Z which is not suppressed by a KM factor but (essentially) only the VEV hierarchy ratio squared, a feature *not* present in **I**. The corresponding Yukawa coupling

$$\lambda_e \bar{e}_R \begin{pmatrix} \nu_L & N_L \\ e_L & E_L \end{pmatrix}_{iI} \begin{pmatrix} h_1^0 & h_2^0 \\ h_1^- & h_2^- \end{pmatrix}_{jJ} \epsilon^{ij} \epsilon^{IJ} + \text{H.c.}, \tag{4}$$

is also seen to generate the electron mass as well as $e - E$ mass mixing via this VEV v_1.

A different Higgs field is needed to generate the exotic fermion masses via the couplings

[5]We note that the fermions in the analogous $SU(2)_I$ situation are also not vector-like under 2_I, but that did not prevent the cancellation of all of the anomalies.

TABLE I. Fermionic Field Content The fermionic content of the theory, including the additional $SU(2)_I$ doublet and triplet fermions D_L and T_L which are necessary to cancel anomalies involving $U(1)_I$. Note that $(d_L h_L)^c$ and $(L_L H_L)$ are doublets of $SU(2)_I$, the latter being a bidoublet under $SU(2)_L \times SU(2)_I$.

$SU(5)$		$SU(3)_C$	T_{3L}	$Y/2$	T_{3I}	$Y_I/2$	Q_D
10	$Q \equiv \begin{pmatrix} u \\ d \end{pmatrix}_L$	**3**	$\begin{pmatrix} 1/2 \\ -1/2 \end{pmatrix}$	1/6	0	0	0
	u_L^c	$\bar{\mathbf{3}}$	0	−2/3	0	0	0
	e_L^c	**1**	0	1	0	0	0
$\bar{\mathbf{5}}$	$L \equiv \begin{pmatrix} \nu \\ e \end{pmatrix}_L$	**1**	$\begin{pmatrix} 1/2 \\ -1/2 \end{pmatrix}$	−1/2	1/2	−1/2	0
	d_L^c	$\bar{\mathbf{3}}$	0	1/3	1/2	−1/2	0
$\bar{\mathbf{5}}$	$H \equiv \begin{pmatrix} N \\ E \end{pmatrix}_L$	**1**	$\begin{pmatrix} 1/2 \\ -1/2 \end{pmatrix}$	−1/2	−1/2	−1/2	−1
	h_L^c	$\bar{\mathbf{3}}$	0	1/3	−1/2	−1/2	−1
5	$H^c \equiv \begin{pmatrix} E \\ N \end{pmatrix}_L^c$	**1**	$\begin{pmatrix} 1/2 \\ -1/2 \end{pmatrix}$	1/2	0	1	1
	h_L	**3**	0	−1/3	0	1	1
1	$\begin{pmatrix} S_2 \\ S_1 \end{pmatrix}_{L,R}$	**1**	0	0	$\begin{pmatrix} 1/2 \\ -1/2 \end{pmatrix}$	−1/2	$\begin{pmatrix} 0 \\ -1 \end{pmatrix}$
1	$D_L \equiv \begin{pmatrix} D^- \\ D^{--} \end{pmatrix}_L$	**1**	0	0	$\begin{pmatrix} 1/2 \\ -1/2 \end{pmatrix}$	−3/2	$\begin{pmatrix} -1 \\ -2 \end{pmatrix}$
1	$T_L \equiv \begin{pmatrix} T^{++} \\ T^{+} \\ T^0 \end{pmatrix}_L$	**1**	0	0	$\begin{pmatrix} 1 \\ 0 \\ -1 \end{pmatrix}$	1	$\begin{pmatrix} 2 \\ 1 \\ 0 \end{pmatrix}$

$$\lambda_h (\bar{h}_R \quad \bar{d}_R)_I h_L (h_3^0 \quad h_4^0)_I + \text{H.c.}, \tag{5}$$

and

$$\lambda_E \begin{pmatrix} \bar{N}_R \\ \bar{E}_R \end{pmatrix}_i \begin{pmatrix} \nu_L & N_L \\ e_L & E_L \end{pmatrix}_{iI} (h_3^0 \quad h_4^0)_J \epsilon^{IJ} + \text{H.c.}, \tag{6}$$

where $H_3 = (h_3^0, h_4^0) \sim (1, 1, 0, 2, -1/2)$, with both neutral members, $h_{3,4}^0$, generally obtaining VEVs, $v_{3,4}/\sqrt{2}$. Here we see that $Q_I(h_3^0) = 0$ so that $v_3 \sim 10$ TeV generates the large N, E and h masses while simultaneously breaking $2_I 1_{I'} \to 1_D$ giving masses to the $W_I^{(\dagger)}$ and Z_I gauge bosons. Since $Q_I(h_4^0) \neq 0$ the VEV $v_4 \sim$ a few GeV or less contributes to the breaking of 1_D (while *not* generating any additional Z–dark photon mixing) and leads to a further contribution to $e - E$ and $d - h$ mass mixing (of the opposite helicity) at the ∼GeV scale. Finally, we note that at this level of discussion (S_2, S_1) can have a bare Dirac mass term, M, consistent with all the $3_c 2_L 1_Y 2_I 1_{I'}$ gauge symmetries. For now it will be assumed that M can be either quite large, of order the scale of 2_I breaking, *or* it might be as small as $\lesssim 1$ GeV, where the DP gets a mass, although this would likely be a very highly tuned value. As mentioned earlier, we could instead choose the potentially more interesting path to make the S_i Majorana fields employing an $SU(2)_I$ triplet in the case when the exotic fields come in two or more generations. Furthermore, perhaps even more interestingly, we could imagine even more complex scenarios where other mass terms exist due to linking the S_i with the other neutral fields ν, N so that we can make interesting models of neutrino masses; this will require additional Higgs fields. However, neither of these paths will be followed here and we leave this for later work. We emphasize that we are free to add additional (vector-like) fermion fields, so long as they do not violate the "finiteness" condition $TrYY_I = 0$. Finally, note that we will also add one new $SU(2)$ singlet, electrically charged scalar, $H_4 \sim (1, 1, 1, 1, 1)$, which (clearly) does not get a VEV, and is introduced solely to ensure that the scalar contributions to $TrYY_I$ vanish in this bottom-up construction, playing no role in the phenomenology below. The various Higgs fields, and their VEVs, are summarized in Table II. Note that the Higgs sector structure just described is somewhat more complex than that seen in the traditional $SU(2)_I$ scenario, though they both have many of the same features.

Now that we have elucidated the necessary set of Higgs fields needed to generate all the fermion masses and the breakings of the necessary gauge symmetries we can write the corresponding potential in the form

TABLE II. Higgs Sector Content The Higgs content required to generate masses for the fermionic content of the theory. The charges under relevant gauge groups are summarized, and the VEV arrangement and approximate scales of the VEVs are listed. The VEVs are assumed to be real.

Φ	$SU(2)_L$	$Y/2$	$SU(2)_I$	$Y_I/2$	$\langle\Phi\rangle$
H_1	**2**	1/2	**1**	0	$\frac{1}{\sqrt{2}}\begin{pmatrix}0\\ v\end{pmatrix}\sim\begin{pmatrix}0\\ 100\text{ GeV}\end{pmatrix}$
H_2	**2**	−1/2	**2**	1/2	$\frac{1}{\sqrt{2}}\begin{pmatrix}v_1 & v_2\\ 0 & 0\end{pmatrix}\sim\begin{pmatrix}1\text{ GeV} & 100\text{ GeV}\\ 0 & 0\end{pmatrix}$
H_3	**1**	0	**2**	−1/2	$\frac{1}{\sqrt{2}}(\,v_3 \quad v_4\,)\sim(\,10\text{ TeV} \quad 1\text{ GeV}\,)$
H_4	**1**	1	**1**	1	0

$$
\begin{aligned}
V = {} & \mu_1^2 H_1^\dagger H_1 + \mu_2^2 \mathrm{Tr}(H_2^\dagger H_2) + \mu_3^2 H_3^\dagger H_3 + \mu_4^2 |H_4|^2 + \lambda_1 (H_1^\dagger H_1)^2 + \lambda_2 [\mathrm{Tr}(H_2^\dagger H_2)]^2 \\
& + \alpha_1 \mathrm{Tr}(H_2^\dagger H_2 H_2^\dagger H_2) + \alpha_2 \mathrm{Tr}(H_2^\dagger H_2 \tilde{H}_2^\dagger \tilde{H}_2) + \lambda_3 (H_3^\dagger H_3)^2 + \lambda_4 |H_4|^4 \\
& + \lambda_5 H_1^\dagger H_1 \mathrm{Tr}(H_2^\dagger H_2) + \lambda_6 H_1^\dagger H_1 H_3^\dagger H_3 + \lambda_7 H_1^\dagger H_1 |H_4|^2 + \lambda_8 H_3^\dagger H_3 \mathrm{Tr}(H_2^\dagger H_2) \\
& + \lambda_9 |H_4|^2 \mathrm{Tr}(H_2^\dagger H_2) + \lambda_{10} H_3^\dagger H_3 |H_4|^2 + \rho H_3 \tilde{H}_2^\dagger H_1 + \rho^* H_1^\dagger \tilde{H}_2 H_3^\dagger,
\end{aligned} \tag{7}
$$

where we have maintained the convention that $H_3 = (h_3^0 h_4^0)$ and $H_1 = (H^+ H^0)^T$, and we have defined $\tilde{H}_2 \equiv \epsilon H_2^* \epsilon$. The phase of the coupling ρ may be absorbed into the relative phases of H_1 and H_3, leaving us with 17 real parameters. From the form of this potential it is obvious that after spontaneous symmetry breaking several fine-tunings in the various parameters are necessary to generate the required hierarchy of the VEVs discussed above.

From this discussion, and as we will see below, it is clear that the dark photon will eventually couple to the SM fields in several ways: (i) via the usual KM $\sim e\epsilon Q$, (ii) via ϵ-unsuppressed mass mixing with the SM Z boson induced by $v_1 \neq 0$ and (iii) via the $v_{1,4} \neq 0$ induced mass mixing of the exotic fermions with their SM partners. Note that the latter two possibilities automatically lead to parity-violating interactions of the dark photon with (some of) the SM fields. If all these effects are of a similar magnitude the nature of the dark photon interactions with the SM fields may be quite different than is usually anticipated.

B. Gauge boson masses and KM

The couplings of the various physical gauge fields to the previously introduced fermions and scalars is determined by both the presence of KM as well as mass mixing among the various weak eigenstates. Based upon the Higgs sector described in the previous subsection, it is straightforward to determine to leading order of the masses of the non-Hermitian gauge fields, i.e., the SM W and the W_I which couple to the two sets of raising and lowering operators of the two $SU(2)$'s; these (diagonal) mass terms are given by

$$
\begin{aligned}
M_W^2 &= \frac{g^2}{4}(v^2 + v_1^2 + v_2^2) \simeq \frac{g^2}{4}(v^2 + v_2^2), \\
M_{W_I}^2 &= \frac{g_I^2}{4}(v_3^2 + v_1^2 + v_2^2 + v_4^2) \simeq \frac{g_I^2}{4} v_3^2,
\end{aligned} \tag{8}
$$

where in the second step we have noted and made use of the large VEV-squared hierarchies $v_3^2 \gg v^2$, $v_2^2 \gg v_{1,4}^2$ based on the suggestive numerical values discussed above. Here we can define the sum $v_{\mathrm{SM}}^2 = v^2 + v_2^2$ for later use below. As in the type II two-Higgs-doublet model (2HDM) [20], we see that v gives mass to the u quarks while v_2 provides mass to the SM d quarks; by analogy, we may write $v = v_{\mathrm{SM}} \sin\beta$ and $v_2 = v_{\mathrm{SM}} \cos\beta$ in familiar notation. Note that W_I can have subleading mixings with the neutral Hermitian gauge bosons, primarily with the dark photon, via the $v_{1,4}$ VEVs that we will discuss further below.

In the case of the real neutral, diagonally coupled gauge bosons, the relevant part of the covariant derivative (suppressing Lorentz indices here) is given in the weak basis by the combination

$$
g T_{3L} W_3 + g_Y \frac{Y}{2} \hat{B} + g_I T_{3I} W_{3I} + g_{Y_I} \frac{Y_I}{2} \hat{B}_I. \tag{9}
$$

Before we can analyze the masses and couplings of the three massive neutral Hermitian gauge bosons in the present setup, we first must remove the effects of KM that arise from a Lagrangian term, now following conventional normalization, of the form (keeping the $w \leftrightarrow I'$ symmetry)

$$
\mathcal{L}_{KM} = \frac{\epsilon}{2 c_w c_I} \hat{B}_{\mu\nu} \hat{B}_I^{\mu\nu}, \tag{10}
$$

where $\hat{B}_{\mu\nu}$ is the field strength of the SM 1_Y gauge field, $\hat{B}_I^{\mu\nu}$ is the corresponding $1_{I'}$ field strength and the finite value of the fermionic contributions to ϵ (which, to be general, we will assume are chiral) are now given in the notation above by

$$\epsilon = c_w c_I \frac{g_Y g_{Y_I}}{24\pi^2} \sum_i \frac{Y_i}{2} \frac{Y_{I_i}}{2} \ln \frac{m_i^2}{\mu^2}. \tag{11}$$

An additional overall factor of $1/2$ is present in the corresponding sum of potential complex scalar contributions. Here we see explicitly that in this setup the exotic vector-like fermions as well as their $SU(2)_I$ (bi)doublet SM partners are *both* playing the role of portal matter fields. In the case of a single generation of exotic fermions we can already evaluate this sum explicitly to find that (treating the Dirac mass of the SM neutrino to be $\sim m_e$ for now)

$$\epsilon = 3.87 \times 10^{-4} \left(\frac{g_I s_I}{g s_w}\right) \left[3 \log \frac{m_E}{m_h} + \log \frac{m_e}{m_d} + \log \frac{m_{H_4}}{m_{H_2}}\right], \tag{12}$$

where the term in the square brackets is $O(1)$ (and likely to be *negative*) since there are no large hierarchies anticipated. Since $\epsilon \sim 10^{-(3-4)}$ we can safely work, most of the time, to leading order in this parameter, removing the KM by the mapping $\hat{B} \to B + \epsilon B_I/(c_w c_I)$ and $\hat{B}_I \to B_I$ and dropping terms of $O(\epsilon^2)$ or smaller. Following this step, it is useful to make the following familiar rotations as the mass eigenstates are not far from the usual SM expectations, with A, Z being the usual SM fields:

$$W_3 = c_w Z + s_w A, \qquad B = c_w A - s_w Z, \tag{13}$$

and correspondingly for the $2_I 1_{I'}$ gauge fields with $s_w \to s_I$, etc. Then the above piece of the covariant derivative, after the removal of KM, can be written as

$$eQA + \frac{g}{c_w}(T_{3L} - s_w^2 Q) Z + e_I \left(Q_I + \eta_2 \frac{Y}{2}\right) A_I + \frac{g_I}{c_I}\left(T_{3I} - s_I^2 Q_I - \eta_1 \frac{Y}{2}\right) Z_I, \tag{14}$$

where here we have used the usual relation $e = g s_w$ (similarly $e_I = g_I s_I$) and defined the η_i parameters to be the combinations of couplings and mixing angles

$$\eta_1 = \frac{\epsilon g s_w s_I}{g_I c_w^2}, \qquad \eta_2 = \frac{\epsilon g s_w}{g_I s_I c_w^2} = \frac{\eta_1}{s_I^2}. \tag{15}$$

To determine the gauge boson masses we recall that the above covariant derivative expression acts on a set of electrically neutral Higgs multiplet members so that $T_{3L}|\text{VEVs}> = -\frac{Y}{2}|\text{VEVs}>$. In the case of Z_I, the η_1 term only acts on Higgs fields which have SM couplings and which have VEVs much smaller than v_3. Since this term is already ϵ suppressed it can be dropped. Thus, to leading order in the small parameters and hierarchical squared VEV ratios, the relevant piece of the covariant derivative acting on Higgs VEVs is simply (recalling that some Higgs carry $Q_I \neq 0$)

$$\frac{g}{c_w} T_{3L} Z + \left(e_I Q_I - \frac{g}{c_w} \epsilon t_w T_{3L}\right) A_I + \frac{g_I}{c_I}(T_{3I} - s_I^2 Q_I) Z_I. \tag{16}$$

Note the familiar form of the dark photon, A_I, coupling to SM matter before mass mixing. The 3×3 symmetric $A_I - Z - Z_I$ mass (squared) matrix can now be written as

$$\mathcal{M}^2 = \begin{pmatrix} (g_I s_I)^2 (v_1^2 + v_4^2) + \frac{g^2}{4c_w^2} \epsilon^2 t_w^2 (v^2 + v_2^2) & \frac{g g_I s_I}{2 c_w} v_1^2 - \frac{g^2}{4c_w^2} \epsilon t_w (v^2 + v_2^2) & M_{13}^2 \\ - & \frac{g^2}{4c_w^2}(v^2 + v_1^2 + v_2^2) & \frac{g g_I}{4 c_w c_I}[(1 - 2s_I^2) v_1^2 - v_2^2] \\ - & - & \frac{g_I^2}{4c_I^2}[v_3^2 + v_2^2 + (1 - 2s_I^2)^2 (v_1^2 + v_4^2)] \end{pmatrix}, \tag{17}$$

and where

$$M_{13}^2 = \frac{g_I^2 s_I}{2 c_I}[v_1^2 + v_4^2](1 - 2s_I^2) + \frac{g g_I}{4 c_w c_I} \epsilon t_w v_2^2. \tag{18}$$

Further note that, e.g., since $v_4^2 \ll v_3^2$, up to corrections of order $(v^2, v_2^2)/v_3^2$, one finds $c_I M_{Z_I} = M_{W_I}$ as expected. While $A_I - Z_I$ mixing is seen to be very highly suppressed by the ratios $v_{1,4}^2/v_3^2 \sim 10^{-(7-8)}$, $Z - Z_I$ and $Z - A_I$ mixing may be of some phenomenological importance. To leading order in the VEV ratios one finds

$$\theta_{ZZ_I} \simeq \frac{g_I/c_I}{g/c_w} \frac{M_Z^2}{M_{Z_I}^2} \frac{v_2^2}{v^2 + v_2^2}, \tag{19}$$

where the last ratio of VEVs is $\cos^2\beta$ in the language above and in the 2HDM, and is $O(1)$, and similarly

$$\theta_{ZA_I} \simeq -\epsilon t_w + \frac{g g_I s_I}{2 c_w} \frac{v_1^2}{M_Z^2} \equiv -\epsilon t_w + \sigma. \tag{20}$$

Thus we see that the SM Z picks up additional suppressed couplings to the "dark" fields via its mixing with both

A_I and Z_I and that the Z_I also picks up an additional coupling to the SM. These couplings are given by the terms

$$\left[g_I s_I Q_I \theta_{ZA_I} + \frac{g_I}{c_I}(T_{3I} - s_I^2 Q_I)\theta_{ZZ_I}\right] Z - \frac{g}{c_w}(T_{3L} - s_w^2 Q)\theta_{ZZ_I} Z_I. \tag{21}$$

These highly suppressed mixing-induced modifications to the SM couplings and the corresponding new couplings to previously "invisible" matter are too small to be presently observable. The corresponding Z mass shift is then to leading order

$$\frac{\delta M_Z^2}{M_Z^2} \simeq -\theta_{ZZ_I}^2 \frac{M_{Z_I}^2}{M_Z^2} = -\gamma \frac{M_Z^2}{M_{Z_I}^2}, \tag{22}$$

where $\gamma > 0$ is a $\lesssim O(1)$ parameter. On the other hand, A_I itself picks up new interactions with the SM fields through its mixing with the Z which, after some algebra, implies that A_I now would couple to the combination

$$g_I s_I Q_I + e\epsilon Q - \sigma \frac{g}{c_w}(T_{3L} - s_w^2 Q). \tag{23}$$

Recall that $e_I = g_I s_I$ is what one usually calls the "dark" coupling, g_D, in an effective field theory approach. Note that the Z-like coupling term, proportional to $\sigma \sim 10^{-4}$ for typical parameter values, is absent in most treatments but arises here due to a Higgs field in the bidoublet carrying both weak isospin and, effectively, a nonzero value of Q_I. Such a term clearly produces parity violation, which can lead to important phenomenological implications. Also, importantly, A_I via $\sigma \neq 0$ now necessarily couples to the SM neutrinos in a generation-independent manner, leading to a potential impact on sensitive neutrino experiments such as DUNE. Correspondingly, due to this mixing, the physical A_I mass to next-to-leading order in the small parameters from the above considerations is

$$M_{A_I}^2 = g_I^2 s_I^2 (v_1^2 + v_4^2) + \sigma(2\epsilon t_w - \sigma) M_Z^2, \tag{24}$$

where the second term, which can sometimes be numerically important for lighter dark photons and can be of either sign, is also new and thus can be of some general significance. To see that both signs are possible in principle, consider the ratio $r_0 = \sigma/(\epsilon t_w)$ so that the coefficient of the M_Z^2 term is just $r_0(2 - r_0)(\epsilon t_w)^2$. Numerically, we indeed find that r_0 can easily be $O(1)$,

$$r_0 \simeq 0.256 \left(\frac{10^{-4}}{\epsilon}\right)\left(\frac{v_1}{1\ \text{GeV}}\right)^2 \left(\frac{g_I s_I}{g s_w}\right), \tag{25}$$

so that the additional term can be negative for some parameter space regions. We note, however, that for dark photon masses $\gtrsim$50–100 MeV and $\epsilon \lesssim 10^{-(3-4)}$ the first term in the expression above is likely to be the far dominant one.

Thus far we have not analyzed the impact of the light VEVs $v_{1,4} \neq 0$. Since these lead to the breaking of $U(1)_D$, thereby generating the A_I mass, the non-Hermitian fields $W_I^{(\dagger)}$ may also mix (slightly) with both the Z_I and A_I by terms such as

$$\frac{g_I^2 s_I v_3 v_4}{2\sqrt{2}}(W_I + W_I^\dagger)(A_I - t_I Z_I). \tag{26}$$

While the Z_I physics we are concerned with here is not at all significantly influenced by this effect, for A_I this mixing induces an additional new coupling term given by

$$-g_I s_I \frac{v_4}{v_3}(T_I^+ + T_I^-), \tag{27}$$

where $T_I^\pm$ are the $SU(2)_I$ raising and lowering operators. Here we see that although A_I mixes with the non-Hermitian W_I and $W_I^\dagger$, it does so in such a way that A_I remains real, as it should. Note that this new interaction is only suppressed by a single power of $v_4/v_3 \sim 10^{-4} \sim \epsilon$, so it can be of some numerical consequence and leads to an off-diagonal coupling between the exotic fermions and their SM partners for the dark photon. Further note that a second term of this type of order $v_1 v_2 / v_3^2$ is also induced, but it is numerically negligible in that the further shift in A_I couplings is only of the order $\sim 10^{-6}$. When both of these W_I and $W_I^\dagger$ terms are *combined* they lead to a *negative* shift in the A_I mass squared $\delta m_{A_I}^2 \simeq -g_I^2 s_I^2 v_4^2$ which is of the same order as discussed already above, resulting in the final leading-order result for the physical A_I mass squared given by

$$M_{A_I}^2 = g_I^2 s_I^2 v_1^2 + \sigma(2\epsilon t_w - \sigma) M_Z^2. \tag{28}$$

As noted above, for the parameter ranges of interest to us we expect that the first term will generally be numerically dominant in this expression.

Without studying the details of the rather complex Higgs potential of this setup described above (which is beyond the scope of the present work) we can make some simple observations with respect to the numbers of degrees of freedom that remain after spontaneous symmetry breaking; the most straightforward case is the number of charged states. H_1 contains one charged state H^+, while the bidoublet H_2 contains two, $h_{1,2}^-$, and one linear combination of these three states must be eaten to supply the longitudinal components of $W_L^\pm$ implying that (including also the state H_4) three charged states remain in the physical spectrum. In the neutral Higgs sector there are a total of ten real fields: five CP-even states and five CP-odd states. In the case of the original five CP-odd neutral

fields, we need to supply longitudinal components to the Z_I, Z, and A_I, which implies that three linear combinations of the CP-odd states become Goldstone bosons. The A_I likely eats some combination of the $Q_I \neq 0$ CP-odd $a^0_{1,4}$ states. The final gauge boson in need of a longitudinal component is $W_I^{(\dagger)}$. Since it carries a nonzero Q_I, $W_I^{(\dagger)}$ must eat both a real CP-even state, likely some linear combination of h^0_4 and h^0_1, as well as a CP-odd state, likely the linear combination of a^0_1 and a^0_4 not eaten by the A_I. Thus, we find that four CP-odd states and one CP-even state become Goldstone bosons, leaving five neutral real scalars remaining in the spectrum, made of some linear combinations of the four uneaten CP-even states and one uneaten CP-odd state. We identify one of these linear combinations, most likely an admixture of the CP-even isodoublet fields within H^0 and h^0_2, with the SM Higgs.

C. Fermion mixing

As was seen in the previous section, the exotic fermions naturally mix with their SM $SU(2)_I$ partners via the same set of Yukawa couplings that generate all of the "diagonal" fermion masses themselves. There are several model-building possibilities here, but for the simplicity of our discussion we will assume that this mixing only occurs with the first generation. It is easy to mutate this into the case where the mixing is dominated by a different generational choice, where multiple families of exotic states exist each mixing primarily with a single SM generation, and the more general case where the mixing can be quite complex. In this simple single-generation case that we consider, e.g., the 2×2 $d - h$ mass matrix in the weak eigenstate basis $\bar{\mathcal{D}}^0_R \mathcal{M}_d \mathcal{D}^0_L$, where $\mathcal{D}^0 = (d^0, h^0)^T$, is given by

$$\mathcal{M}_d = \begin{pmatrix} m^0_d & m^0_h \frac{v_4}{v_3} \\ m^0_d \frac{v_1}{v_2} & m^0_h \end{pmatrix}, \tag{29}$$

where we have defined $m^0_{d,h} = \lambda_{d,h} v_{2,3}/\sqrt{2}$ employing the notation above. Clearly since the off-diagonal elements are "small," straightforward algebra leads to $m^0_{d,h} \simeq m_{d,h}$, which are the corresponding physical particle masses, to a very good approximation. This mass matrix is easily diagonalized, as usual, via the biunitary transformation $M_D = U_R \mathcal{M}_d U_L^\dagger$, where M_D is diagonal so that $\mathcal{D}_{L,R} = U_{L,R} \mathcal{D}^0_{L,R}$ are the mass eigenstates. Note that U_L is determined via the relation $M_D^2 = U_L \mathcal{M}_d^\dagger \mathcal{M}_d U_L^\dagger$ while U_R is similarly determined via $M_D^2 = U_R \mathcal{M}_d \mathcal{M}_d^\dagger U_R^\dagger$. To leading order in the small parameters corresponding to VEV ratios from above we then find that

$$U_L \simeq \begin{pmatrix} 1 & -\frac{m^0_d}{m^0_h}\frac{v_1}{v_2} \\ \frac{m^0_d}{m^0_h}\frac{v_1}{v_2} & 1 \end{pmatrix}, \tag{30}$$

implying that U_L is numerically very close to the unit matrix (which we will assume from now on) since the off-diagonal term is $\sim O(10^{-8})$ or less, while for U_R we find instead to this same order in the small parameters

$$U_R \simeq \begin{pmatrix} 1 & -\frac{v_4}{v_3} \\ \frac{v_4}{v_3} & 1 \end{pmatrix}, \tag{31}$$

where, as we saw above, $\theta_R \simeq -v_4/v_3$ is of order ϵ, and can be phenomenologically important. Note that these same conclusions would hold if h mixed with any of the three SM generations. A very similar result is obtained in the case of $e - E$ mixing with identical results as above, but with the interchange $U_L \leftrightarrow U_R$. These results are qualitatively similar to what was obtained in **I** and lead to similar phenomenological implications as we will discuss below.

We now see that the combined effect of the A_I coupling term $\sim(T_I^+ + T_I^-)$ discussed in the last subsection above and the fermion mixing seen here now yields an effective exotic-SM *off-diagonal* coupling for the dark photon that is not explicitly ϵ suppressed and is given by

$$-2 g_I s_I \frac{v_4}{v_3} (\bar{h} \gamma_\mu d_R + \bar{d} \gamma_\mu h_R) A_I^\mu, \tag{32}$$

with a similar result holding in the case of, e.g., $e - E$ mixing with $m_h \to m_E$ and with $R \to L$ in the expressions above. Here we see that this coupling is roughly of order ϵ, as will generally be assumed in the phenomenological analysis below and as was anticipated in **I**. From this expression we can determine the induced coupling of the longitudinal component of A_I to this current structure as well as that of the associated Goldstone boson by employing the equivalence theorem [21]. Approximating $m_{A_I} = g_I s_I v_1$ in our mass range of interest (given the arguments above), we find that the overall strength of this interaction, λ, is given by

$$\begin{aligned} \lambda &= -\left(\frac{v_4}{v_1}\right)\left(\frac{2 m_h}{v_3}\right) \\ &= -0.3 \left(\frac{v_4}{v_1}\right)\left(\frac{m_h}{1.5\ \text{TeV}}\right)\left(\frac{10\ \text{TeV}}{v_3}\right) \sim O(1), \end{aligned} \tag{33}$$

especially if $v_4 > v_1$ which can easily happen. This is semiquantitatively similar to what we obtained in **I** for the toy model we constructed there. As was found there, this implies that decays such as $h \to d A_I$ or $E \to e A_I$ via the A_I's longitudinal component experience no ϵ-like suppression and will be completely dominant over other anticipated processes such as $h \to dZ, H$ and $h \to uW$. The fact that λ is $O(1)$ leads to numerous phenomenological implications, some of which were hinted at in **I**. Explicitly, the Goldstone boson associated with A_I, i.e., G_{A_I}, has an off-diagonal coupling given by

$$i\lambda(\bar{h}d_R - \bar{d}h_L)G_{A_I}, \tag{34}$$

with an analogous term, e.g., for $E-e$-type interactions with the opposite helicity structure. It is easy to see that the physical CP-even scalar state(s) containing a significant $\mathrm{Re}h_4^0$ component will also have off-diagonal, SM-exotic fermion couplings of very similar strength, i.e., $\sim\lambda(\bar{h}d_R + \bar{d}h_L)S$, as was found in the toy model presented in **I**. This state would essentially be the real, CP-even partner to the CP-odd A_I's associated Goldstone boson above. In the limit where the $2_I 1_{I_Y}$ breaking scale becomes large, as in the toy model case, we would expect that this real scalar state, S, is light, $\lesssim$ a few GeV, and with a mass set by the $U(1)_D$ breaking scale. Without a detailed study of the Higgs potential of the present setup shown above (which is comparable in complexity in our case to, e.g., that of the left-right symmetric model with Dirac neutrinos [22], though here there is no left-right symmetry relating the 17 free parameters in the potential), which is beyond the scope of the present work, we will assume that the vacuum structure of the potential allows this state to be present in the spectrum with the anticipated mass and couplings as in **I**.

The introduction of vector-like fermions which mix with SM fermions via Yukawa couplings, as outlined above, may induce new flavor-changing neutral currents (FCNCs) through, e.g., the SM Z boson coupling. FCNCs in this context have been studied in the literature [23–25], and are proportional to products of the VLF-SM Yukawa couplings and the ratio of the SM VEV to the VLF mass, $\lambda_i\lambda_j^* v^2/M^2$. The case here is slightly different, however, as the mixing between the VLF and the SM fermions are only non-negligible for the SM fermion which transforms the same way under the SM gauge groups as the VLF, i.e. above we have $d_R - h_R$ and $e_L - E_L$ mixing but no $d_L - h_L$ or $e_R - E_R$ mixing at order ϵ. Since the fermions which experience mass mixing couple identically to the Z, there are no Z-mediated FCNCs in this model at order ϵ.[6] Nevertheless, we see that there are FCNCs that are also mediated by the dark photon A_I which we will briefly discuss, using the down-like quark sector as an example.

The most general flavor structure of this model has an additional set of VLFs for each generation, so that the relationship between the mass eigenstates and the gauge eigenstates, $\mathcal{D}_R = U_R\mathcal{D}_R^0$, becomes a mixing between six states which may be written in block form as

$$U_R \simeq \begin{pmatrix} D_R & -\frac{v_4}{v_3}U_{R,12} \\ \frac{v_4}{v_3}U_{R,21} & H_R \end{pmatrix}, \tag{35}$$

where D_R mixes the SM down-like quarks with themselves, H_R mixes the VLFs with themselves, and $U_{R,12}$ and $U_{R,21}$ mix the SM and VLF components. We have defined the SM-VLF mixing blocks with a prefactor of $v_4/v_3 \simeq 10^{-4}$ to emphasize the small mixing between the SM and VLF states, so $U_{R,12}$ and $U_{R,21}$ may have components which are of order unity. This mass mixing induces tree-level FCNC couplings between the down-like quarks and the A_I, given by

$$g_I s_I A_I^\mu \bar{\mathcal{D}}_{Ri}\gamma_\mu V_{ij}^I \mathcal{D}_{Rj}, \tag{36}$$

where V^I is a 6×6 matrix which may be written in block form as

$$V^I \simeq \begin{pmatrix} \frac{v_4^2}{v_3^2}U_{R,12}U_{R,12}^\dagger & -\frac{v_4}{v_3}U_{R,12}H_R^\dagger \\ -\frac{v_4}{v_3}H_R U_{R,12}^\dagger & H_R H_R^\dagger \end{pmatrix}. \tag{37}$$

Since the A_I is much lighter than the SM Z, it may be produced on shell in meson decays, which could provide constraints on the flavor sector of these models. As an example, we consider the tree-level processes $b\to s + A_I$, $b\to d + A_I$, and $s\to d + A_I$, with a long-lived A_I which escapes the detector. These decays mimic the SM processes $B\to K\nu\bar{\nu}$, $B\to\pi\nu\bar{\nu}$, and $K\to\pi\nu\bar{\nu}$, respectively, and thus may be constrained by limits on the branching fractions of these decay channels. We estimate the branching fractions for the corresponding new physics processes $B\to KA_I$, $B\to\pi A_I$, and $K\to\pi A_I$ using the hadronic form factors of Refs. [26,27], taking $m_{A_I} = m_{\mathrm{light}}$, the mass of the light meson in the decay product, and assuming $g_I^2 s_I^2 \simeq 0.1$. Our estimates of these branching fractions and the current limits are summarized in Table III.

From these estimates we see that the observed branching fraction of $K^+\to\pi^+\nu\bar{\nu}$ imposes sizable constraints on the flavor structure of the model, requiring either a flavor structure such that $|(U_{R,12}U_{R,12}^\dagger)_{sd}|^2 \lesssim 10^{-8}$, which can happen if, e.g., $U_{R,12}\lesssim 10^{-2}$, or that the decay be kinematically inaccessible with $m_{A_I} > 350$ MeV in order to trivially avoid the constraint. The constraints from B decays are comparatively weaker, with a relatively mild flavor suppression factor $|(U_{R,12}U_{R,12}^\dagger)_{bd}|^2 \lesssim 0.1$ proving sufficient to evade the bound on $\mathcal{B}(B^+\to\pi^+\nu\bar{\nu})$, and the bound on $\mathcal{B}(B^+\to K^+\nu\bar{\nu})$ providing little constraint, even for $|(U_{R,12}U_{R,12}^\dagger)_{bs}|^2 \sim O(1)$.

We note that FCNCs may also impact neutral meson oscillations, but due to the light mass of the A_I these effects are difficult to estimate, and an analysis of the impact of weakly coupled FCNCs with light mediators on neutral meson oscillations is beyond the scope of the present work. Further, we note that a similar set of A_I-mediated FCNCs will be present in the lepton sector, which could be probed by, e.g., $\mu\to e$ measurements, though the rate would be

[6]We note that Z-mediated FCNCs do occur due to mixing in the left-handed down-like quark sector, but as noted in the above analysis of U_L, we expect these terms to be $O(10^{-(10-16)})$, depending on the mass of the down-like quark, and we will neglect these couplings.

TABLE III. FCNC Branching Fraction Estimates vs. SM Bounds Tree-level estimates of A_I-mediated FCNC branching fractions were made using the hadronic form factors of Refs. [26,27], assuming $m_{A_I} = m_{\text{light}}$, the mass of the light meson in the decay product, and $g_I^2 s_I^2 \simeq 0.1$.

Tree-level estimate	Current SM limit
$\mathcal{B}(K^+ \to \pi^+ A_I) \sim 3 \times 10^{-3} \lvert(U_{R,12} U_{R,12}^\dagger)_{sd}\rvert^2$	$\mathcal{B}(K^+ \to \pi^+ \nu\bar{\nu}) = (1.7 \pm 1.1) \times 10^{-10}$ [28]
$\mathcal{B}(B^+ \to K^+ A_I) \sim 8 \times 10^{-6} \lvert(U_{R,12} U_{R,12}^\dagger)_{bs}\rvert^2$	$\mathcal{B}(B^+ \to K^+ \nu\bar{\nu}) < 1.6 \times 10^{-5}$ [29]
$\mathcal{B}(B^+ \to \pi^+ \nu\bar{\nu}) \sim 6 \times 10^{-5} \lvert(U_{R,12} U_{R,12}^\dagger)_{bd}\rvert^2$	$\mathcal{B}(B^+ \to \pi^+ \nu\bar{\nu}) < 1.4 \times 10^{-5}$ [29]

suppressed by a factor of $\epsilon^2 v_4^4 / v_3^4 \sim 10^{-24}$ at least. Decays forbidden in the SM, such as $K^+ \to \pi^+ \mu^+ e^-$, could also provide a very clean probe of the FCNCs discussed here, though this rate would be further suppressed by a factor of $O(10^{-16})$ relative to the $K^+ \to \pi^+ A_I$ discussed above.

IV. SURVEY OF SOME BOTTOM-UP PHENOMENOLOGY

Given the rich structure we have introduced above, we might expect that this setup will have a complex phenomenology which has partial overlap with both the $SU(2)_I$ models and the conventional dark photon picture, perhaps augmented by some of what we discussed previously in **I**. The first and most obvious topic to address is how the physics of the new heavy gauge bosons and exotic fermions differs from the more familiar and well-studied $SU(2)_I$ from E_6-inspired models. One certain issue we need to address is the nature of the interplay between the exotic and SM sectors: is there a single set of exotic states that primarily mixes with the corresponding fields in a single SM generation (and which one is it, e.g., do we have dominant $h-d$, $h-s$ or $h-b$ mixing?) or is there a set of exotic fields corresponding to each generation? In traditional E_6-inspired models the answer is clear, while here we see that there are several different possibilities which lead to somewhat different phenomenology. In the discussion that follows we will ignore issues related to flavor-changing processes and consign such discussions to later work.

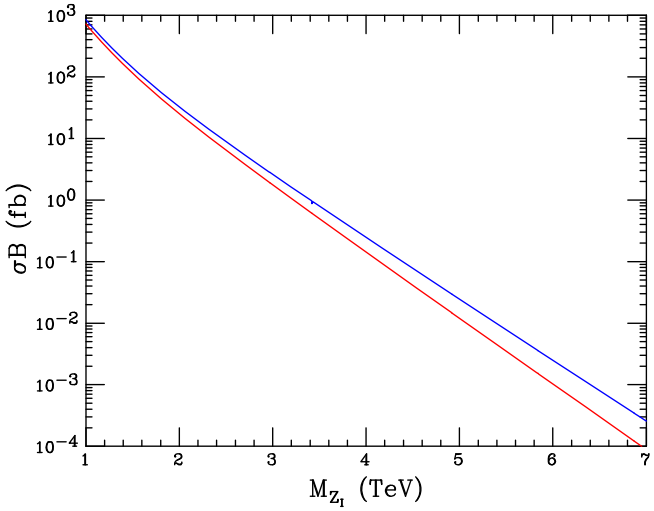

FIG. 1. σB_ℓ for Z_I production at the $\sqrt{s} = 13$ (red) and 14 (blue) TeV LHC where only decays to SM fields are assumed to be kinematically allowed and with $r = \frac{g_I/c_I}{g/c_w} = 1$ being assumed. Here the Z_I is assumed to couple universally as in the original most well-studied scenario.

These model-dependent differences make themselves felt in even the simplest production process, i.e., that of Z_I production in the Drell-Yan channel when the Z_I can only decay to SM final states with the most trivial difference being the overall Z_I coupling strength which in E_6 models is proportional to $\sim\sqrt{\frac{5 s_w^2}{3}}$ due to GUT coupling requirements. Here, the overall coupling is set by g_I/c_I so that Z_I production cross sections can be determined up to an overall factor of $r = (g_I/c_I)/(g/c_w)$ which we expect to be $O(1)$.[7] Of course, a potentially more significant difference is whether the Z_I couples only to $d\bar{d}$, $s\bar{s}$ or $b\bar{b}$ initial states (or all three) and whether it will appear in only the e^+e^-, $\mu^+\mu^-$, or $\tau^+\tau^-$ channels (or, again, all three). For example, we are reminded that in the more well-studied case, there is a universality of interactions among the generations so that all three initial states as well as all three final states will contribute to the potential Z_I Drell-Yan cross section and corresponding decay signatures at the LHC. In the present situation, all of these scenarios need to be explored independently.

The simplest situation, and the one that allows us to make most direct contact with previous studies, is the production of Z_I with identical couplings to all three SM generations but which is kinematically forbidden to decay into any of the exotic vector-like fermions or into $W_I W_I^\dagger$. In such a case, σB_ℓ in the narrow-width approximation is shown in Fig. 1 assuming that $r = \frac{g_I/c_I}{g/c_w} = 1$; note that the overall cross section in this case is independent of the value of x_I (since SM states all have $Q_I = 0$) and that it is simply proportional to r^2 so that other cases are easily obtained by a simple overall rescaling. As can be seen from this figure, the present ATLAS null searches [30] employing 139 fb^{-1} of 13 TeV integrated luminosity exclude Z_I masses below $\simeq$5.2 TeV under this set of assumptions. A similar null

[7] In what follows we will employ the narrow-width approximation for our Z_I analyses.

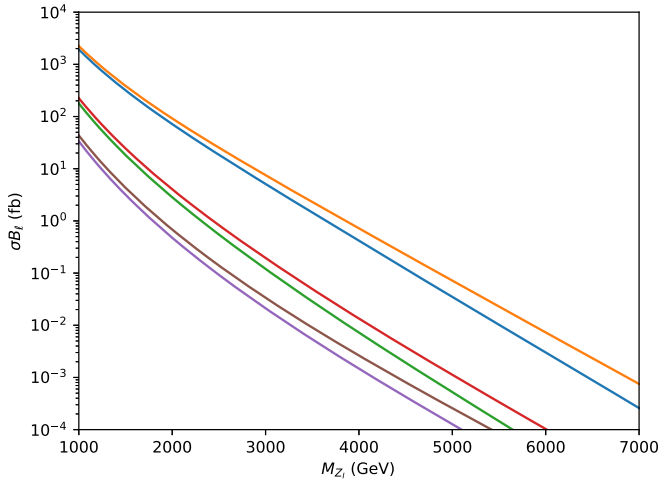

FIG. 2. σB_ℓ for Z_I production at the $\sqrt{s} = 13$ (lower) and 14 TeV (upper) LHC for each pair of curves assuming that the Z_I only couples to a single SM generation and decays to exotic partners are forbidden, taking $r = 1$. From top to bottom, the Z_I couples to the first, second, and third generation of the SM, respectively.

search performed at the 14 TeV HL-LHC with 3 ab^{-1} of luminosity [31] would increase the exclusion limit on a Z_I to masses below $\simeq$5.9 TeV under the same set of assumptions.

A second possibility, as discussed above, is that only a single set of exotic fermions exist which mix with a particular SM generation. In such a case only a single SM generation couples to Z_I and so only the searches in a particular dilepton channel are applicable for setting constraints. Thus, e.g., if only the third generation carries nonzero $2_I 1_{I'}$ quantum numbers, the relevant process to examine is then $b\bar{b} \to Z_I \to \tau^+\tau^-$. We first consider the simplest case where the Z_I still cannot decay to any of the exotic states so that the cross section remains x_I independent with only an overall sensitivity to the coupling ratio r as above. The production rates for this case at the $\sqrt{s} = 13$ and 14 TeV LHC are shown in Fig. 2.[8]

Figure 3 then shows how these Z_I production cross sections in the various dilepton channels translate into current LHC search limits and the expectations for the HL-LHC assuming either universal couplings or coupling to only one of the SM generations. In order to obtain these results in the case of the $\tau^+\tau^-$ third-generation couplings, we have recast the results from an ATLAS $b\bar{b} \to H \to \tau^+\tau^-$ study[32,33] making corrections for the acceptance differences between spin-0 and spin-1 resonances.

[8]Here, and in what follows, we will ignore the possible effects of small intergenerational fermion mixings which could result in flavor-changing dark currents. Note that in the quark case this involves possible intergenerational mixings among the right-handed fields which are not well probed by SM measurements and may even be absent in some scenarios.

It is interesting to explore how these results change as we move further away from these rather vanilla scenarios. In addition to variations in the overall coupling, i.e., $r \neq 1$, the Z_I may also decay into one or more exotic fermion final states and also into $W_I W_I^\dagger$ which would modify the branching fraction for the leptonic decay mode used in the search. Furthermore, the Z_I may *not* couple universally, perhaps only to $d\bar{d}$, $s\bar{s}$ or $b\bar{b}$ initial states and consequently only leptonically decay to e^+e^-, $\mu^+\mu^-$ or $\tau^+\tau^-$ final states, respectively, as we saw above. In such cases one also needs to employ the individual constraints as applicable to each of these final states as previously considered [30].

When the Z_I is sufficiently massive it can also decay into some if not all of the exotic non-SM states; the partial widths for these decays, unlike those to SM final states, will explicitly depend upon the value of x_I. Furthermore, once $x_I > 0.75$ the $Z_I \to W_I W_I^\dagger$ channel also opens up via the usual non-Abelian trilinear coupling. The main effect of these new decay modes of the Z_I for our discussion is to reduce the value of the relevant leptonic branching fraction, B_ℓ, and thus a correspondingly reduced signal rate resulting in a suppression of the search/exclusion reach. This effect, however, is expected to be relatively mild over most of parameter space as B_ℓ is reduced by at most a factor of $\simeq$6.8, even in the extreme case when all three generations of exotic states (without much phase-space suppression) as well as $W_I W_I^\dagger$ are allowed to contribute to the total Z_I width, and this maximum reduction only occurs when $x_I \simeq 1$. Figure 4 gives us a feel for how large a reduction in B_ℓ may occur where, for purposes of demonstration in the universal case, we have included decays into three generations of degenerate $N, E, h, S_{1,2}$ states as well as $W_I W_I^\dagger$ for $x_I > 0.75$. Very similar reduction factors will also occur in the cases where there is only a single generation of exotics which mix with only a single SM generation. From Fig. 4 we see that the typical leptonic branching fraction seen here will have very little influence on the Z_I search reach at the HL-LHC.

Perhaps at a similar level of relative "simplicity" is the direct pair production of the exotic fermions h, E, N, etc., which themselves may be accessible to LHC experiments. As in **I**, once produced h will dominantly decay into its associated SM partner $q = d$, s or b, which will appear as a jet, plus A_I or S which produce either missing transverse energy (MET) or lepton-jet signatures. h, being a color triplet, is certainly pair produced via QCD from, at leading order (LO), $q\bar{q}$, gg annihilation, as is the case for the top quark as well as other more familiar vector-like quarks. For the $\sqrt{s} = 13$ TeV LHC the cross section due to these processes is given in **I** while for the case of $\sqrt{s} = 14$ TeV [34,35] the slightly larger cross section is shown in Fig. 5 with the caveat here that no additional, nonelectroweak interactions are present; this caveat needs some explanation. As discussed in **I**, the decay of $h\bar{h}$ are not those of

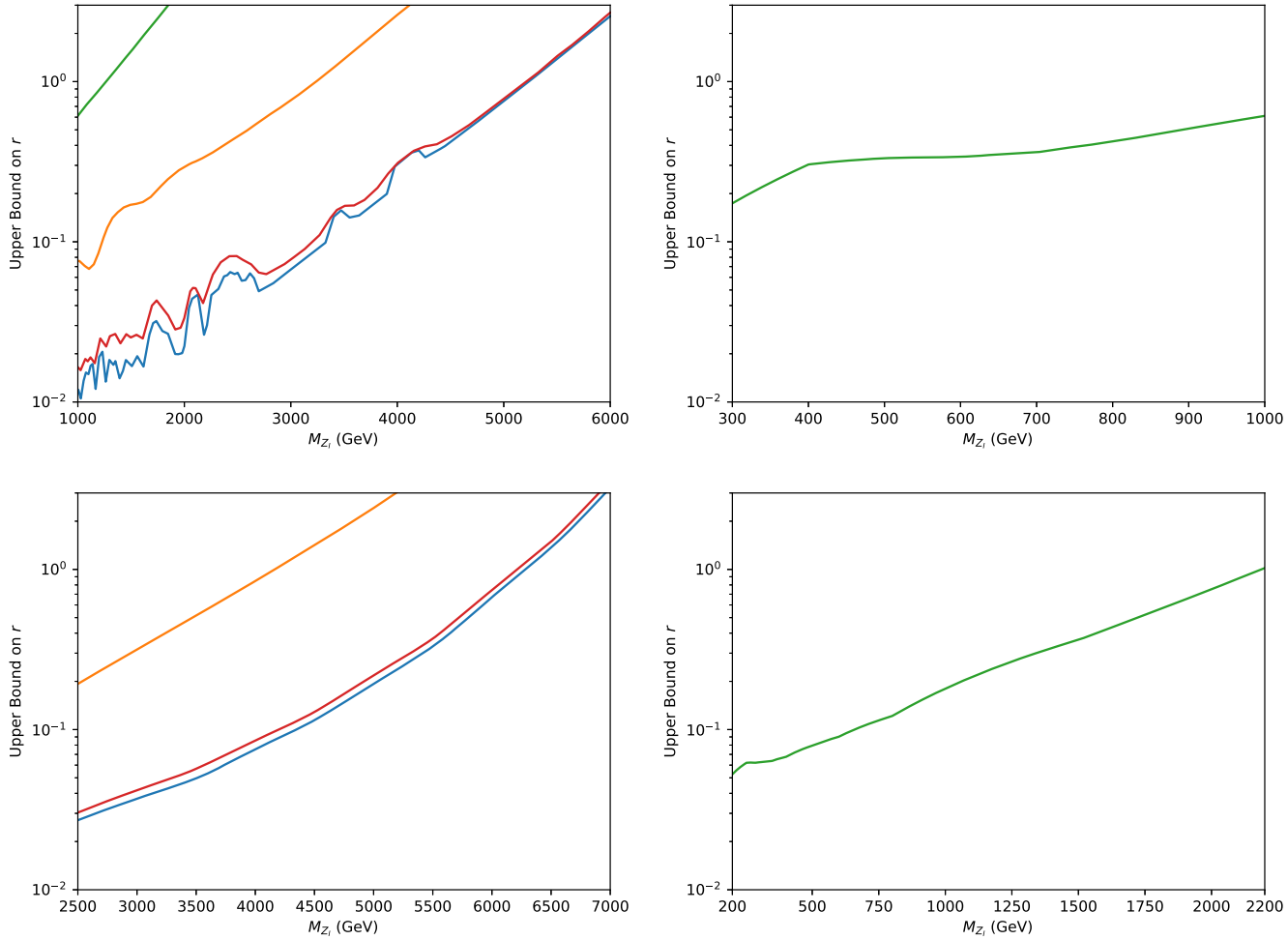

FIG. 3. (Top left) Limits from the $\sqrt{s} = 13$ TeV LHC on the values of the parameter r as described in the text, as a function of the mass of the Z_I, employing the results from ATLAS searches for dilepton decays [30,32]. From left to right the curves correspond to only third-generation couplings (green), only second-generation couplings (gold), universal couplings (red), and only first-generation couplings (blue). (Top right) Extension of the results in the previous panel for the case of third-generation couplings to lower Z_I masses. (Bottom left) Same as the top left panel, but now employing an ATLAS analysis assuming a null result at the HL-LHC with $\sqrt{s} = 14$ TeV and $L = 3$ ab^{-1} [31]. (Bottom right) Corresponding limit in the $\tau^+\tau^-$ case employing the ATLAS heavy Higgs study [33] with acceptance corrections included for a spin-1 state.

conventional vector-like states but instead will lead to two, non-back-to-back jets plus MET, if A_I/S are very long lived, or lepton jets [36–38] if the decays occur inside the detector. Decays of A_I/S far from the detector may be captured by specialized experiments looking for long-lived states [39,40] such as FASER and MATHUSLA.

While the $gg \to h\bar{h}$ process is left unaltered by the additional interactions described above, the $q\bar{q} \to h\bar{h}$ process may be significantly modified when $q = d$, s or b via a t-channel longitudinal A_I exchange (or equivalently, the G_{A_I} Goldstone boson) as well as that due to the corresponding light CP-even scalar, S, provided that the parameter λ is sufficiently large. In a similar vein, the t-channel W_I exchange may also produce a potentially important contribution but it is suppressed by both the relatively small $SU(2)_I$ gauge coupling as well as the large mass of the W_I itself; the neglect of this contribution at this level of discussion is similar to the neglect of Z exchange in the case of top pair production within the SM context. Clearly, the numerical impact of these new exchanges will differ significantly depending upon which SM quark mixes with the exotic partner h. To quantify this possibility, consider the modification to the $q\bar{q} \to h\bar{h}$ differential cross section at LO, where we will neglect the masses, $\lesssim 1$ GeV, of the exchanges in the t channel compared to other mass scales in the process. Defining the coupling ratio $\chi = \lambda^2/(4\pi\alpha_s)$, with λ as given above, and defining $z = \cos\theta^*$, with θ^* being the partonic center-of-mass frame scattering angle, we find, for the quark that mixes with h, that

$$\frac{d\sigma}{dz} = \frac{\pi\alpha_s^2\beta}{9\hat{s}}\left(B_1 + 2\chi B_2 + \frac{9}{2}\chi^2 B_3\right), \tag{38}$$

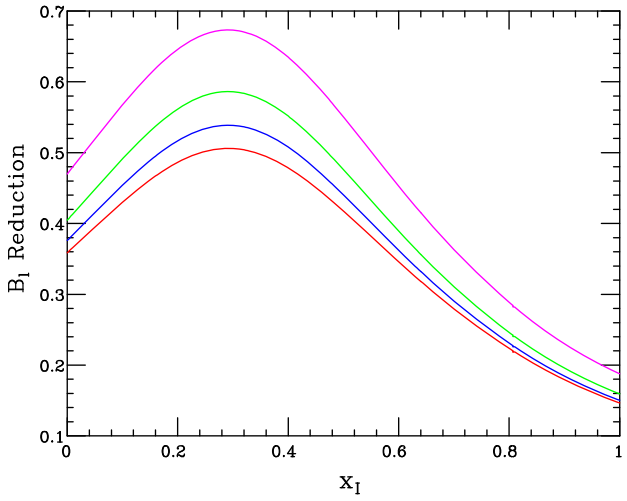

FIG. 4. Multiplicative B_ℓ suppression factor for the Z_I as a function of x_I due to the additional non-SM decays into three generations of degenerate exotic fermions plus $W_I W_I^\dagger$ (for $x_I > 0.75$) as discussed in the text. From bottom to top the curves assume $m_{\rm exotic}/m_{Z_I} = 0$, 0.2, 0.3 and 0.4, respectively.

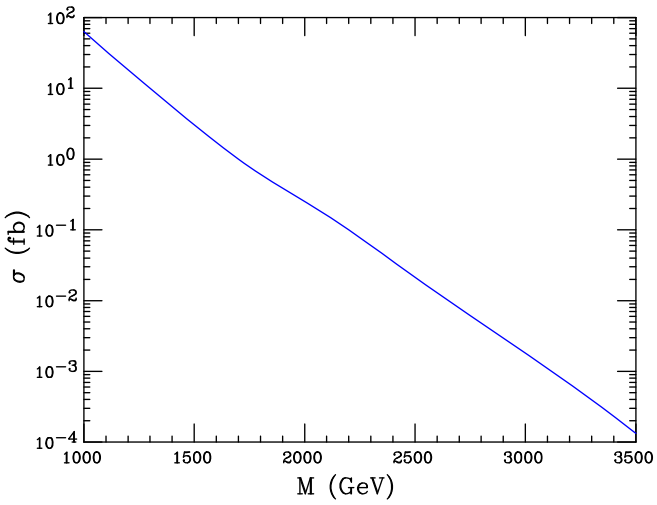

FIG. 5. Pure QCD NNLO $h\bar{h}$ production cross section at the $\sqrt{s} = 14$ TeV LHC as a function of m_h using HATHOR following Ref. [34].

where $\beta^2 = 1–4m_h^2/\hat{s}$, and where

$$B_1 = 2 - \beta^2(1 - z^2), \qquad B_2 = \frac{(1-\beta z)^2 + 1 - \beta^2}{(1+\beta^2)/2 - \beta z},$$
$$B_3 = \frac{(1-\beta z)^2}{[(1+\beta^2)/2 - \beta z]^2}, \tag{39}$$

with B_1 being the conventional LO pure QCD result. The impact of this exchange will not only depend on the value of λ, but even more importantly on which of the $q = d$, s, b initial-state quarks participates in the mixing with h since their parton densities are all quite different. As we will see, not only is h ($\bar{h}$) production pushed more forward (backward) due to this t-channel exchange as one might expect, but the overall total $h\bar{h}$ production cross section also increases, in some cases significantly.

To get an idea of the impact of $\lambda \neq 0$ for the various nonuniversal $q = d$, s, b choices, we have taken the LO $q\bar{q}$ and gg processes and reweighted them by K factors to recover the corresponding next-to-next-to-leading-order (NNLO) SM total cross section result when they are combined and $\lambda = 0$ is assumed[34,35]. Figure 6 shows these modifications to the $h\bar{h}$ angular distributions for the three nonuniversal choices assuming $m_h = 1.5$ TeV at the 14 TeV LHC, and taking rather large values of λ for purposes of demonstration. Here we see the obvious result that for any fixed value of λ the overall impact of the t-channel exchange increases dramatically as the choice of q goes from b to s to d. For example, in the case $q = b$, a substantial impact is only found when λ is quite large $\simeq 3$. However, for $q = d$, we see that a reasonable impact is seen even for values of λ less than unity. In all cases, as expected, we see that the impact is largest in the forward direction due to the t-channel nature of the exchange. Since the QCD aspects of heavy vector-like quark production are well known [34], a measurement of the *total* cross section for $h\bar{h}$ production would perhaps give us a rough indication of the value of λ in some cases. Figure 7 shows the total $h\bar{h}$ cross section at 14 TeV as a function of λ for the three choices $q = b$, s, d. Here we see that noticeable effects may be visible for $\lambda \simeq 3$, 1 and 0.3, respectively, for these three cases.

Unlike for the QCD color triplet exotic fermion h, N and E form a vector-like SM weak isodoublet so they can only be produced via the $2_L 1_Y 2_I 1_{I'}$ interactions. Apart from possible resonant production in the decay of the Z_I and W_I gauge bosons (as was discussed above and will be discussed further below), SM $W^\pm$ exchange provides the largely dominant, model-independent production mechanism at the LHC: Z-mediated production is smaller by roughly an order of magnitude.[9] The rate for this process as a function of $m_E (= m_N)$ for both the $\sqrt{s} = 13$ and 14 TeV LHC is shown in Fig. 8, where the possible effects of $\lambda \neq 0$ have been ignored. Here we see that such states may be visible out to masses $\sim$1.5 TeV, depending on their decays and the relevant SM backgrounds. As noted above and in **I**, these differ from the vector-like leptons usually discussed, i.e., $E \to eA_I, S$ rather than $E \to eH, eZ, \nu W$. However, present limits from the LHC on vector-like leptons with these "conventional" decay paths are, and may likely continue to be, rather poor due to large SM backgrounds except in the case where they mix with the τ [42].

[9]For some range of masses gg-induced off-shell Z, Z_I contributions may also be significant [41] here but we will neglect this possibility in this brief discussion.

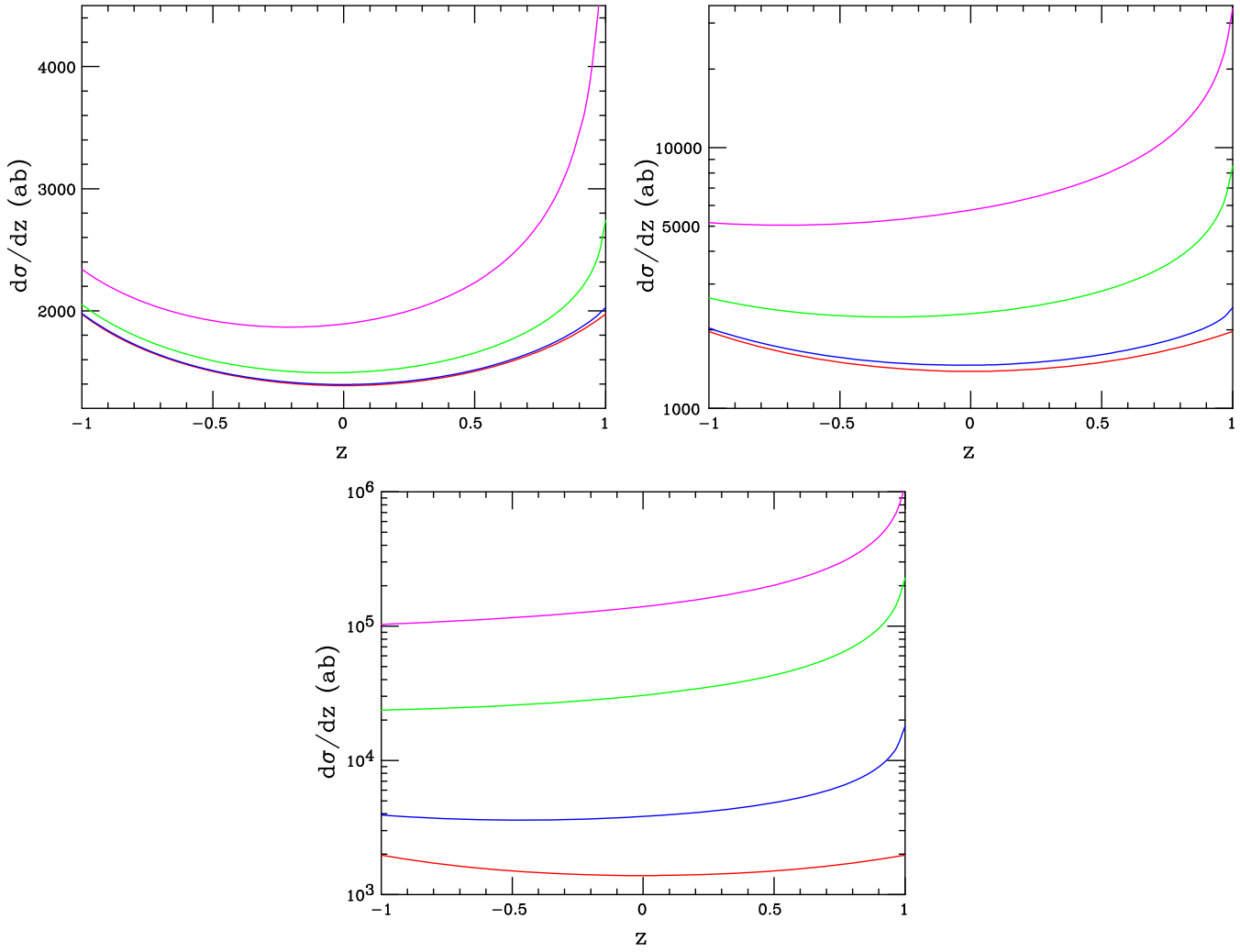

FIG. 6. (Top left) Angular distribution for $h\bar{h}$ production at the 14 TeV LHC assuming $m_h = 1.5$ TeV and where the h's SM partner is the b quark. From bottom to top the curves assume that $\lambda = 0, 1, 2, 3$, respectively. (Top right) Same as the previous panel but now taking the h's SM partner to be the s quark. (Bottom) Same as the previous panel but now taking the h's SM partner to be the d quark. Very similar distributions are obtained when, e.g., $m_h = 2$ TeV is assumed.

We now turn to the production of the W_I gauge boson; there are several possible mechanisms for this in the present setup, one of which does not occur in any form in the usual traditional treatment. In the original $SU(2)_I$ scenario [15], it was noted that since W_I coupled an exotic vector-like fermion to a SM one it could not be singly produced at colliders in the usual Drell-Yan fashion, the only options then being pair production via $q\bar{q}$ annihilation, which we will further discuss below, or in association with an h via gluon-quark fusion, i.e., $qg \to hW_I$ where $q = d$, s, b. In the present setup, this represents three distinct possibilities. The LO subprocess differential cross section for this reaction can be easily extracted from the result given long ago (in a somewhat different context) in Ref. [43] with a few obvious alterations, such as $u \to d$, assuming coupling to the first SM generation, $W_R \to W_I$, etc., including a rescaling by an overall factor of g_I^2/g^2. The resulting cross sections as a function of the W_I mass for various choices of m_h are shown in Fig. 9. The two upper panels correspond to the cases where $q = d$ for $\sqrt{s} = 13$ and 14 TeV, respectively, while the lower panels are for 14 TeV with $q = s$ or b, respectively; in all cases one sees that a large part of the model parameter space is potentially accessible for all choices of q at $\sqrt{s} = 14$ TeV. Once $W_I h$ is produced, $h \to qA_I, qS$ (with $q = d$, s or b) as discussed above and, if $m_{W_I} > m_{h,E}$, then $W_I \to hq, Ee$ with h, E then decaying as previously described.[10] For $W_I h$, this final state is somewhat similar to that for $h\bar{h}$ production as discussed above (which provides a significant background) but with an extra jet which if not b tagged could be easily mimicked by QCD initial-state radiation. Within that region of parameter space

[10]If W_I is less massive than h (or E, N etc.) it could possibly decay into a three-body final state as will be discussed below.

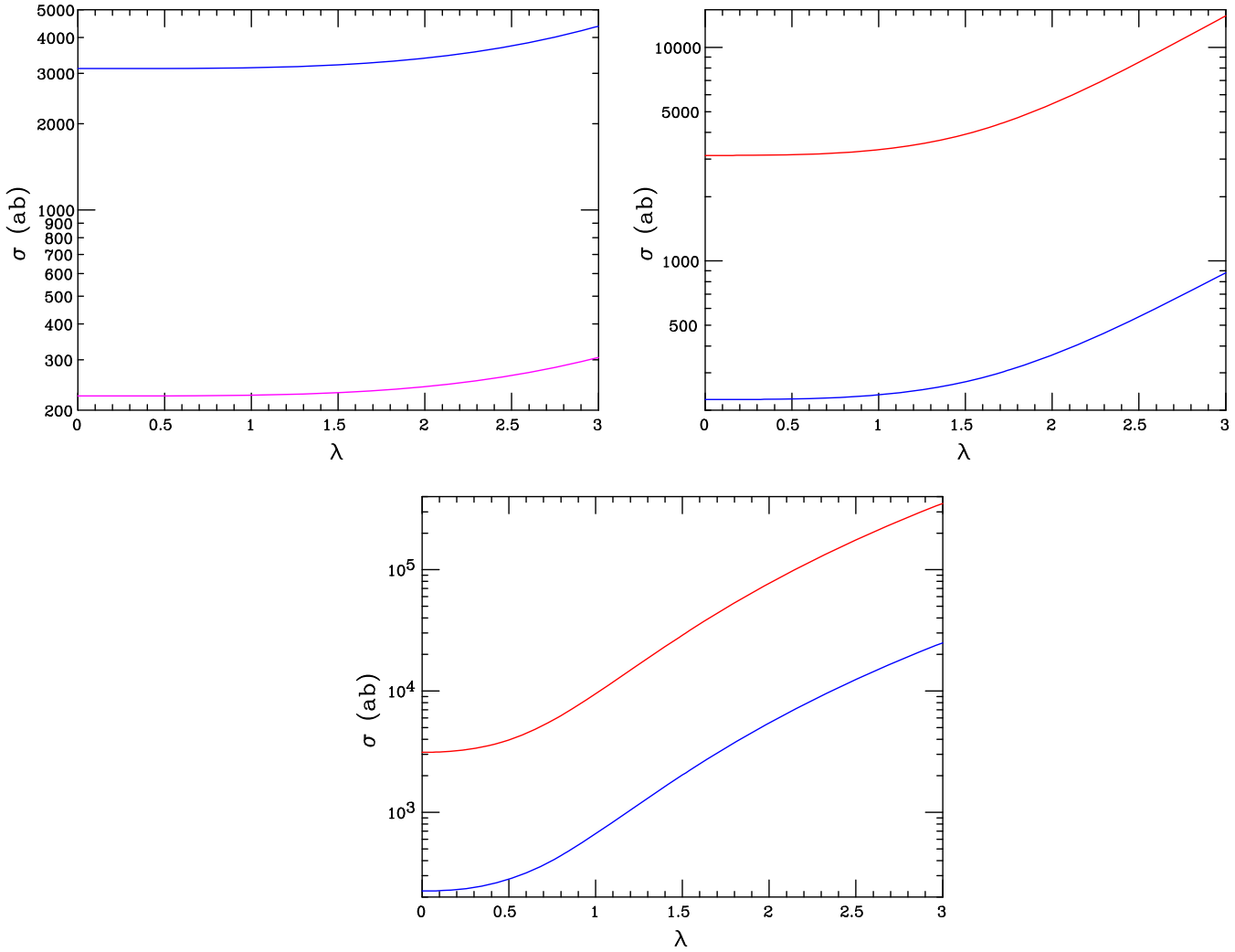

FIG. 7. (Top left) Total cross sections corresponding to the angular distributions for $h\bar{h}$ production at 14 TeV shown in the previous figure but now as a function of λ and assuming that $m_h = 1.5$ (2) TeV for the top (bottom) curve. Here $h - b$ mixing is assumed. (Top right) Same as the previous panel but now taking the h's SM partner to be the s quark. (Bottom) Same as the previous panel but now taking the h's SM partner to be the d quark.

where V, S decay inside the detector so that the h's can be reconstructed, the corresponding reconstruction of the W_I mass peak using the extra q jet would substantially reduce the QCD background. This production process requires further study.

Another possibility that is more model dependent (and thus we only briefly mention it here) is that the two SM singlet states $S_{1,2}$ might be relatively light with the $Q_I = -1$ state, S_1, split from and slightly heavier than the $Q_I = 0$ state, S_2, by $2_I 1_{I'}$ gauge boson loops. In this scenario, if these states are indeed light, W_I can always decay into them. The $S_2 - S_1$ mass splitting, being radiatively generated, is rather small so that if both states are light S_1 will generally be relatively long lived due to the three-body nature of the decay over most of the parameter space. Hence, it may likely appear that S_1 is stable on detector length scales given the significant boost from the large W_I mass. In such cases this final state appears as $W_I \to \text{MET}$ at a collider detector, implying that $h - W_I$ associated production may likely produce a monojet signature due to the $h \to qA_I, S$ decay. Of course, this scenario may be altered once any significant mixings among all the neutral fields are taken into account.

W_I may also be produced in pairs at the LHC. Since the W_I is electrically neutral and carries no weak SM charges and also $Q_I(d) = 0$, the dominant pair-production process $q\bar{q} \to W_I W_I^\dagger$, proceeds via s-channel Z_I exchange as well as h exchange in the t channel (whose amplitudes destructively interfere to satisfy unitarity as $s \to \infty$). This is similar to the SM W^+W^- process, but without the photon contribution and with a massive neutrino. We recall that only two independent mass parameters, m_h and m_{W_I}, enter into the cross section for this process since $M_{W_I} = M_{Z_I} c_I$ at tree level in this setup. However, we note that both the values of (the overall factor of) $(g_I/g)^4$ and

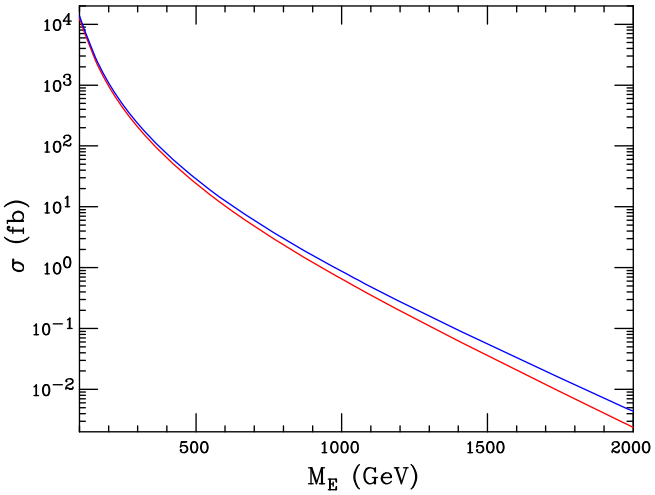

FIG. 8. $q\bar{q} \to W^{\pm *}_{\rm SM} \to E\bar{N} + N\bar{E}$ production cross section at the $\sqrt{s} = 13$ (red) and 14 TeV (blue) LHC as a function of $m_N = m_E$.

of $x_I = s_I^2$ are both undetermined in the bottom-up approach that we are following here. Recall that the traditional pure $SU(2)_I$ limit of the current setup is achieved in the $x_I \to 0$ limit so that the additional $U(1)$ is then decoupled. Furthermore, in the present setup, this cross section will be highly sensitive to the choice of $q = d, s, b$ as we saw in the case of several other production processes above. The full differential subprocess cross section for this reaction can be extracted, with some care, from the detailed analysis presented in Ref. [44]. A final "variable" in this calculation is the width of Z_I which enters into the s-channel exchange and is particularly important for the range $x_I > 3/4$ where $Z_I \to W_I W_I^\dagger$ can occur on shell as discussed above. For a reasonable set of choices of exotic fermion mass variations, we generally find that Γ_{Z_I}/M_{Z_I} usually lies in the range ~0.01–0.03 when g_I/g is not far from unity, which we will assume in the numerical analysis that follows.

Defining as above $\beta^2 = 1\text{–}4M_{W_I}^2/\hat{s}$ and with $z = \cos\theta^*$, one finds the subprocess cross section to be given by

$$\frac{d\sigma}{dz} = \frac{g_I^4}{g^4}\frac{G_F^2 M_W^4}{12\pi}\frac{\beta}{\hat{s}}\left(E_2 + \frac{-2\hat{s}(\hat{s} - m_{Z_I}^2)I + A\hat{s}^2}{(\hat{s} - M_{Z_I}^2)^2 + (m_{Z_I}\Gamma_{Z_I})^2}\right), \quad (40)$$

where the functions $E_2, I, A(\hat{s}, \hat{t}, \hat{u})$ were given in Ref. [44] with

$$\hat{t}, \hat{u} = m_{W_I}^2 - \frac{\hat{s}}{2}(1 \mp \beta z). \quad (41)$$

Cross sections for this process at the 14 TeV LHC are shown in Figs. 10 and 11, which show some of the detailed model parameter dependence for this process. As noted, these can depend quite strongly on the value of x_I as it determines the $Z_I - W_I$ mass relationship and thus whether or not the $Z_I \to W_I W_I^\dagger$ process can happen on shell and is thus resonantly enhanced. Since on-shell Z_I production has already been discussed above, here we will *mostly* be interested in the case where $x_I < 0.75$. In Fig. 10 we see that for values of $x_I \lesssim 0.6$–0.7, away from the potential Z_I contribution, the cross section is only weakly dependent on x_I. We see in the top left panel that, not unexpectedly, as we increase m_h we essentially turn off the destructive s-/t-channel interference and the cross section rises, reaching an asymptotic value due to the Z_I exchange diagram alone.[11] For this same range of x_I, with m_h held fixed, the upper right panel shows that the production rate falls rapidly with increasing m_{W_I} in a manner which is, again, relatively insensitive to the specific value of x_I. The lower panel shows the rather strong x_I sensitivity to the properties of the Z_I resonance once the on-shell decay process $Z_I \to W_I W_I^\dagger$ becomes allowed.

Similarly to the other production processes considered, this cross section depends upon the choice of $q = d, s, b$. Figure 11 shows this cross section as a function of m_{W_I} for various values of m_h while holding $x_I = 0.25$ fixed but varying the choice of $q = d, s, b$ at the 14 TeV LHC. Here we see that, e.g., assuming $m_h = 1$ TeV and demanding a target cross section of at least 10 (1) ab for purposes of demonstration, m_{W_I} is restricted to be $\lesssim$1.7(2.2), 1.4 (1.9) and 1.1 (1.5) TeV, respectively, assuming $q = d, s, b$. Clearly, we see that the associated production channel generally provides the largest signal rate for W_I production provided that the value of m_h is not too large.

Once the $W_I^{(\dagger)}$ is produced its main decay paths are back into a SM-exotic fermion pair, e.g., $\bar{e}E(e\bar{E}), \bar{\nu}N(\nu\bar{N})$ or $\bar{S}_2 S_1(S_2\bar{S}_1)$ and $\bar{d}h(d\bar{h})$.[12] These two-body partial widths are completely fixed by the W_I and $h, E/N$, etc., masses apart from an overall factor of g_I^2/g^2. However, it is always possible that $m_{E,N}$ and/or m_h are larger than m_{W_I} so that such decay modes are blocked.[13] Of course through the previously discussed fermion mass-mixing effects, governed by $\theta \sim 10^{-4}$, decays into e^+e^- and/or $d\bar{d}$ are always allowed, but with partial widths that are highly suppressed by $\theta^2 \sim 10^{-8}$. Much larger partial widths are potentially possible via the off-shell, three-body modes such as $W_I \to eE^* \to e^+e^-(d\bar{d})A_I/S$, where here A_I is essentially the longitudinal mode, i.e., the Goldstone boson G_{A_I}. These are suppressed by relative three-body factors of $\sim\lambda^2/16\pi^3$, which prove not to be too prohibitive, and asymptotically

[11]The asymptotic cross section value as $m_h \to \infty$ with $m_{W_I} = 1(5)$ TeV is roughly ~25% larger than that when $m_h = 5(10)$ TeV.

[12]Here e, ν, d are being used to represent any of the corresponding fermions of the three SM generations.

[13]However, if the bare mass M is sufficiently small then the $\bar{S}_2 S_1$ mode will always remain open.

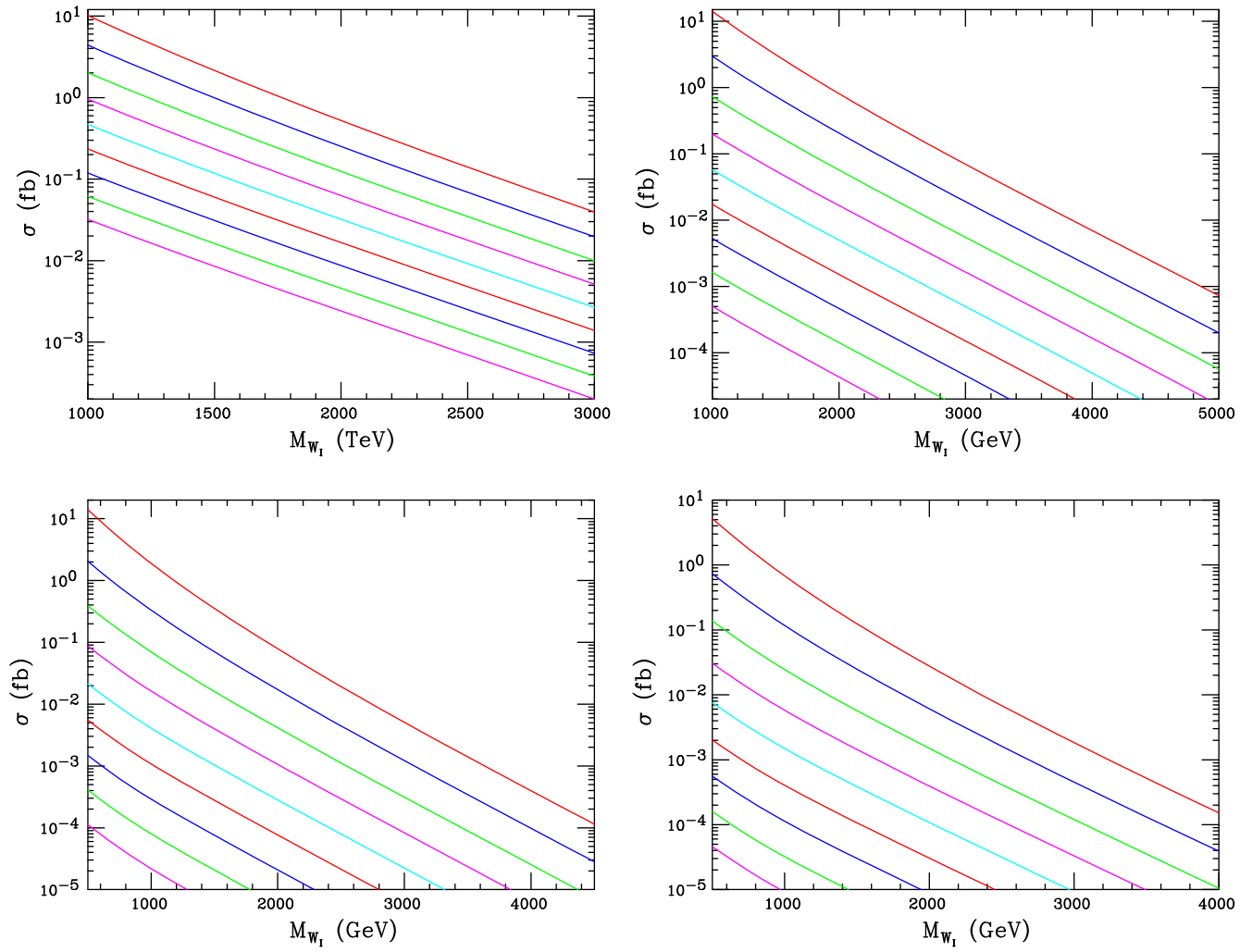

FIG. 9. (Top left) $gd \to hW_I + \text{H.c.}$ associated production cross section, taking $(g_I/g)^2 = 1$, as a function of the W_I mass assuming, from top to bottom, that $m_h = 1, 1.25, \ldots, 3$ TeV, respectively, at the 13 TeV LHC with d being the h's SM partner. (Top right) Same as the previous panel but now for 14 TeV LHC and for $m_h = 1, 1.5, \ldots 5$ TeV. (Bottom left and bottom right) Same as the previous panel but now assuming that s (b) is the SM partner coupling to h, respectively.

scale as $\sim(m_{W_I}/m_E)^2$. Figure 12 shows the reduced partial width for this decay process, in units of $g_I\lambda/g$, as a function of $\delta = m_E/M_{W_I}$; an analogous result is obtained in the case of h exchange except for an additional multiplicative factor of ~ 3 for color and QCD corrections.

In the present setup, W_I can also be produced by a new mechanism not present in the classic $SU(2)_I$ scenario. Since A_I contains a small admixture of $W_I + W_I^\dagger$, the process $q\bar{q} \to W_I^{(\dagger)} A_I/S + \text{H.c.}$ via t-channel h exchange, with $q = d$, s, or b becomes possible via $\lambda \neq 0$; again, we see that it is the longitudinal component of A_I (or, equivalently, the Goldstone boson G_{A_I}) that is mainly responsible for this reaction. This process has a kinematical advantage over both $W_I W_I^\dagger$ and $W_I h$ production in that only a single heavy particle needs to be produced in the final state and thus it can lead to the largest signal cross section for W_I production in some parameter space regions. Also, unlike the pair production case, the amplitude is proportional to the product λg_I instead of g_I^2; this can be especially advantageous if λ is indeed large. The subprocess cross section for this reaction is given (in the limit where the dark photon and light scalar masses can be safely neglected) by

$$\frac{d\sigma}{dz} = \left(\frac{\lambda^2 g_I^2}{g^2}\right) \frac{G_F m_W^2}{96\sqrt{2}\pi\hat{s}} \frac{m_h^2}{m_{W_I}^2} \left(1 - \frac{M_{W_I}^2}{\hat{s}}\right) \frac{A + 1 - \beta^2 z^2}{[1 - \beta z + C]^2}, \tag{42}$$

where here $\beta = (\hat{s} - m_{W_I}^2)/(\hat{s} + m_{W_I}^2)$, $z = \cos\theta^*$ as above and

$$A = \frac{4m_{W_I}^2 \hat{s}}{(\hat{s} + M_{W_I}^2)^2}, \qquad C = \frac{2(m_h^2 - m_{W_I}^2)}{\hat{s} + m_{W_I}^2}. \tag{43}$$

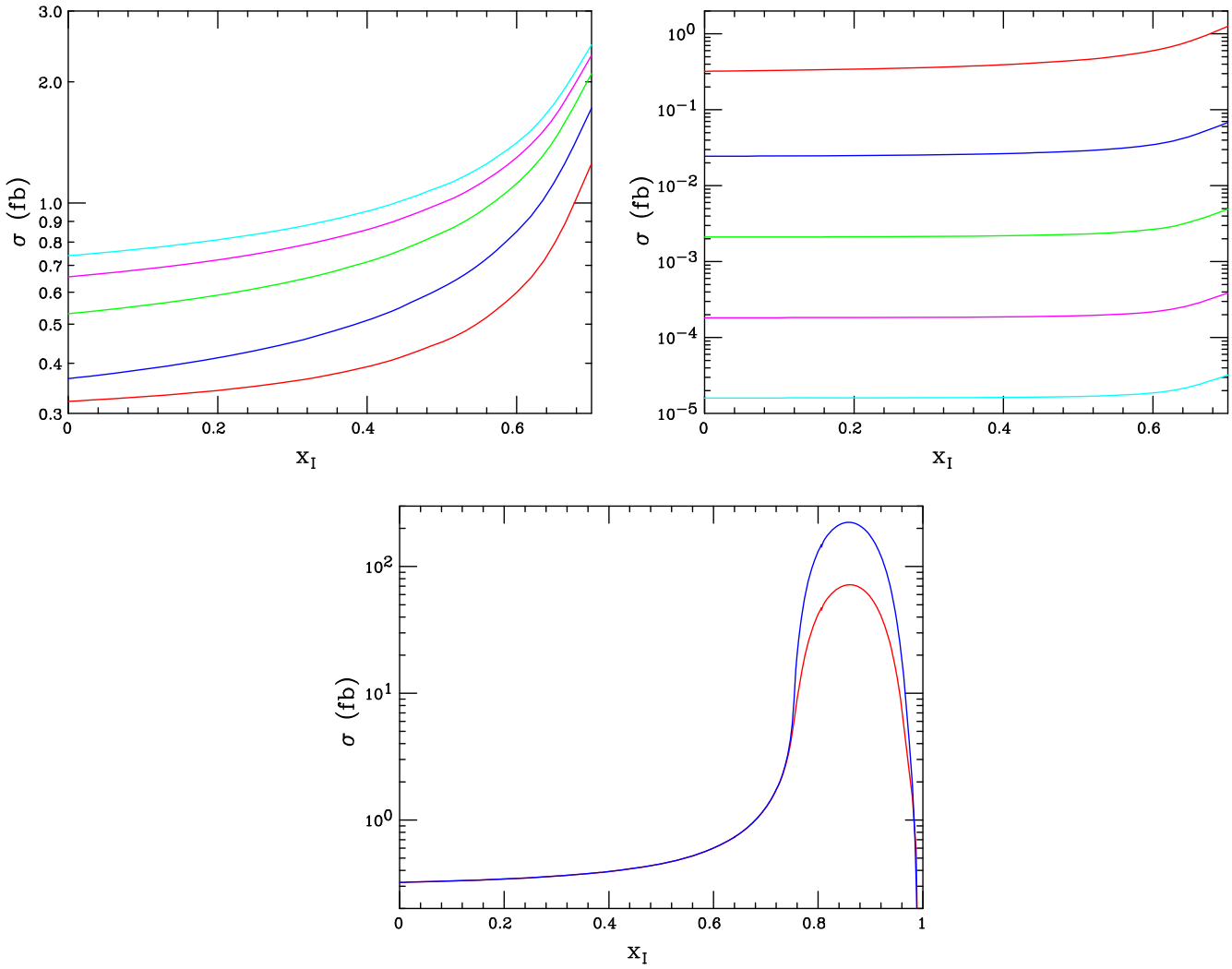

FIG. 10. (Top left) $q\bar{q} \to W_I W_I^\dagger$ total cross section at the 14 TeV LHC as a function of $x_I = s_I^2$ assuming $M_{W_I} = 1$ TeV and, from bottom to top $m_h = 1, 2, \ldots, 5$ TeV, respectively, with d being the h's SM partner. Here an overall scaling by $(g_I/g)^4$ is still required as in the case of associated production. (Top right) Same as the previous panel but now with $m_h = 1$ TeV and, from top to bottom, $m_{W_I} = 1, 1.5, \ldots, 3$ TeV, respectively. (Bottom) Same as the previous panel but now assuming $m_{W_I} = m_h = 1$ TeV and including the Z_I resonance region at large x_I assuming that $\Gamma_{Z_I}/m_{Z_I} = 0.01$ (0.03), shown as the top blue (bottom red) curve.

The resulting cross section for this new associated production process as a function of m_{W_I} is shown in Fig. 13 for all three choices of initial-state SM quark $q = d$, s or b. Here we see that, e.g., if $\lambda g_I/g \simeq 1$ then cross sections of at least 10 (1) ab are obtained for $m_{W_I} \lesssim 3.9(4.9)$ TeV assuming $q = d$. This is a substantially larger reach than found in the case of pair production, but is somewhat inferior to the rates found in the case of hW_I associated production under the same assumptions. For comparison, the corresponding results for the cases $q = s$ and $q = b$ are $m_{W_I} \lesssim 2.5(3.5)$ and $\lesssim 2.0(2.9)$ TeV, respectively. Depending upon the W_I decay mode, this final state can also easily lead to MET-, monojet- or monolepton-type signatures, although lepton jets are possible when the A_I decays sufficiently rapidly.

Finally, we consider the $q\bar{q} \to 2A_I(2S)$ production process which proceeds via t- and u-channel h exchanges. In the case of the A_I final state this is by far dominated by the longitudinal polarization mode, and so is well represented by the production of the corresponding Goldstone boson. Summing over both final states and neglecting the A_I, S masses in comparison to other mass scales, the subprocess differential cross section for this identical particle final-state process is given by

$$\frac{d\sigma}{dz} = \frac{\lambda^4}{48\pi\hat{s}} \frac{z^2(1-z^2)}{(a^2-z^2)^2}, \tag{44}$$

where $a = 1 + 2m_h^2/\hat{s}$ and $z = \cos\theta^*$. Note that the outgoing A_I/S states will generally appear at large p_T and not

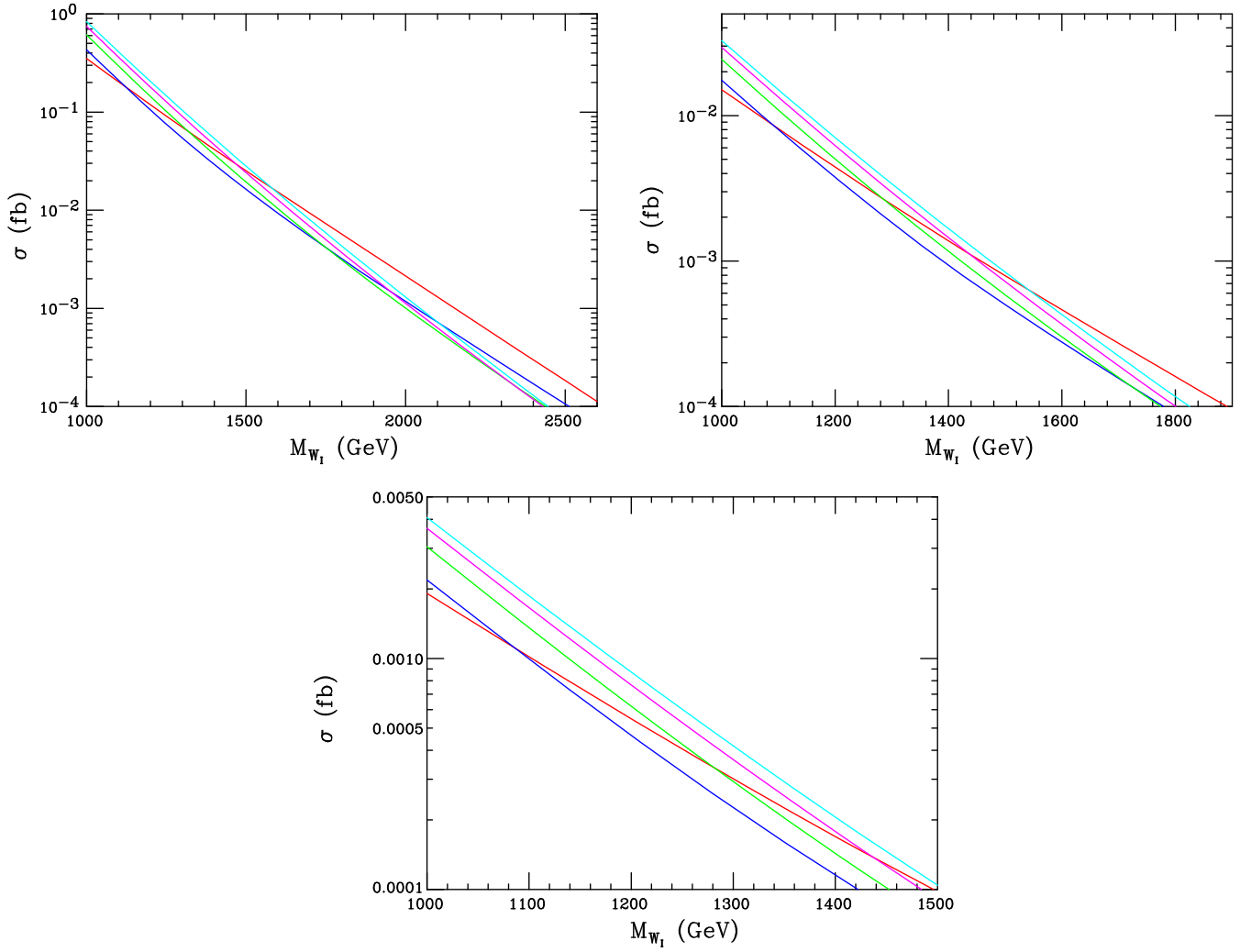

FIG. 11. (Top left) Same as in the previous figure but now assuming that $x_I = 0.25$ and displayed as a function of m_{W_I} with, from bottom to top at the left axis, $m_h = 1, 2, \ldots, 5$ TeV. (Top right and bottom) Same as the previous panel but now assuming that s or b is the SM partner to h, respectively.

along the beam directions. Examining the numerator, we see that in the limit of large m_h this cross section is pure d wave, as we might expect from the production of pairs of identical spin-0 particles in the final state; this is the result of the destructive interference between the t-channel and u-channel exchange amplitudes. The resulting integrated cross section is shown in the lower left panel of Fig. 13 for the different choices of $q = d, s, b$, as above. This result is numerically smaller than might be expected for the pair production of two very light states due to this strong destructive interference, and we see that in the large-m_h limit this interaction turns into an effective dimension-eight operator. For the analogous $q\bar{q} \to A_I S$ process, where constructive interference now occurs instead, one obtains the resulting $\sim p$-wave cross section

$$\frac{d\sigma}{dz} = \frac{\lambda^4}{24\pi\hat{s}} \frac{a^2(1-z^2)}{(a^2-z^2)^2}, \tag{45}$$

which is seen in the lower right panel of Fig. 13 as a function of m_h for the different choices of $q = d, s, b$. Here, unlike in the case of $2S$ or $2A_I$ production, we see a substantial event rate qualitatively similar to our naive expectations. As in the case of pair production, we note that the outgoing A_I/S states will generally appear at large p_T and not along the beam directions.

For both of these processes on their own, unlike the others considered previously, one sees the potential lack of an obvious signal to trigger on at the LHC if the A_I/S is sufficiently boosted so that it decays far outside the detector. In such a case one must rely on the production of an extra jet(s) produced by QCD to act as a trigger to produce a monojet signature. Even in the case where A_I/S decay inside the detector, this additional radiation may act as a useful trigger.

In order to analyze the production of monojet events at the 13 TeV LHC, we use FeynRules [45] to produce UFO

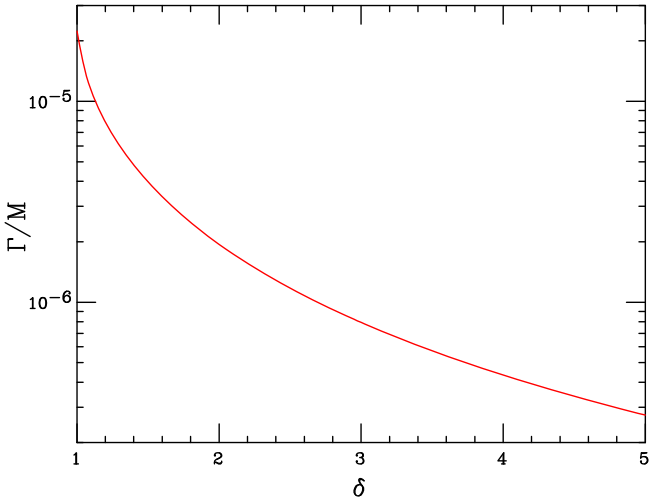

FIG. 12. Reduced partial width, Γ/m_{W_I}, for the process $W_I \to \bar{e}E^* \to e^+e^-A_I/S$ as a function of $\delta = m_E/m_{W_I}$ and in units of $(g_I\lambda/g)^2$. Apart from a color factor of 3, a suitable redefinition of both λ, δ and a small correction from QCD, a similar partial decay rate would be obtained for the $W_I \to \bar{d}h^* \to d\bar{d}A_I/S$ process.

files that may be passed to MadGraph5_aMC@NLO [46] in order to generate parton-level events. We generate events for $2A_I$, $2S$, and $A_IS + 1 - 3$ generator-level jets final states, as all of these subprocesses will produce large missing E_T, though the $2A_I$ and $2S$ final states are suppressed by the destructive interference between the t and u channels as discussed above. It is important to include the additional generator-level hard jets in the final states, as these allow for processes with qg, $\bar{q}g$, and gg initial states to contribute to the $E_T^{\rm miss}$ + jets signal, though they do not contribute to the exclusive $2A_I$, $2S$, A_IS production considered above. At the generator level, we require the leading jet to have $p_{T,j1} > 150$ GeV and that $E_T^{\rm miss} > 150$ GeV, and that all jets have $p_{T,j} > 20$ GeV. We employ the five-flavor number scheme (5FNS), treating the b quark as massless and including it in the proton parton distribution function, and calculate the production cross section at leading order. These parton-level events are then showered and hadronized within PYTHIA8 [47]. We use the MLM matching scheme in order to avoid double counting jets from the parton-level generation and the parton showering procedure, using the merging parameters **xqcut** = 20 GeV and **QCUT** = 30 GeV. In order to compare generated events to present searches, we use DELPHES 3 [48] to simulate detector effects, and make the cuts on the final states as outlined in the most recent ATLAS search [49]. In particular, the leading jet must have $p_{T,j1} > 250$ GeV and $|\eta| < 2.4$, $E_T^{\rm miss}$ must be at least 250 GeV (this is the requirement for the IM1 search in Ref. [49]; the subsequent IM2-IM10 searches have successively higher cuts on $E_T^{\rm miss}$), there must be no electrons with $p_T > 20$ GeV, no muons with $p_T > 10$ GeV, and there may be at most four central jets with $|\eta| < 2.8$ and $p_T > 30$ GeV in the event. The left panel of Fig. 14 shows the signal cross section at the 13 TeV LHC after the IM1 cuts have been applied as a function of the mass of the down-like quark partner h, for the cases of h coupling individually to each of $q = d$, s, b as well as the universal coupling case, taking $\lambda = 1$ in all cases. The coupling to the first generation dominates the production cross section in the universal case, and the two are nearly equal for $m_h \gtrsim 3$ TeV.

Since the cross section scales as λ^4, the 36.1 fb^{-1} ATLAS monojet search can be used to constrain λ for the various coupling scenarios. Using the tightest limit on the signal cross section from the IM1-IM10 searches of Ref. [49], we place an upper bound on λ for each coupling scenario as a function of the h mass, shown in the right panel of Fig. 14. We note that the searches with higher missing E_T thresholds tend to be more constraining, with the IM7 search, corresponding to $E_T^{\rm miss} > 700$ GeV, being the most constraining for $m_h = 1$ TeV, and the IM10 search, with $E_T^{\rm miss} > 1$ TeV, becoming the tightest constraint as m_h increases. The constraints on λ from this search are not very stringent, especially at larger m_h and for the cases of h coupling to the second and third generations. For $m_h = 1$ TeV, we find an upper limit $\lambda < 0.49$ for the universal coupling case, while the upper limits on λ for h coupling to d, s, and b are 0.59, 0.76, and 0.81, respectively. These limits weaken considerably as m_h increases, as can be seen in Fig. 14. One may expect increased sensitivity in this search channel at the $\sqrt{s} = 14$ TeV HL-LHC, but even a gain of ~23 in sensitivity only translates to a factor of ~2.2 in $\lambda_{\rm max}$, since the cross section scales as λ^4.

V. DARK MATTER?

An issue that we have not yet addressed is the identity of the DM state in the present setup.[14] By definition, we require that this DM state be a stable, SM singlet which predominantly couples to the SM via the dark photon and, hence, must necessarily have $Q_D \neq 0$. Among the set of exotic fermions introduced in our discussion so far, we see that the $Q_D = -1$ state S_1, which sits in an $SU(2)_I \times U(1)_{Y_I}$ isodoublet and is vector-like with respect to this gauge group, would naturally fulfill these basic desired requirements. Considered in isolation, S_1, together with S_2, will have a common Dirac mass, M, but radiative corrections will split these two states with the S_1 state ending up being the *heavier* of the two and thus disqualifying it as a stable DM possibility. Since $Q_D(S_2) = 0$, it too is not a DM candidate since it does not couple to A_I. Furthermore, given

[14]For simplicity in the discussion that follows, we will consider only the simpler situation of a single set of exotic fermions that mix/couple to only one of the SM generations but the discussion can be directly generalized.

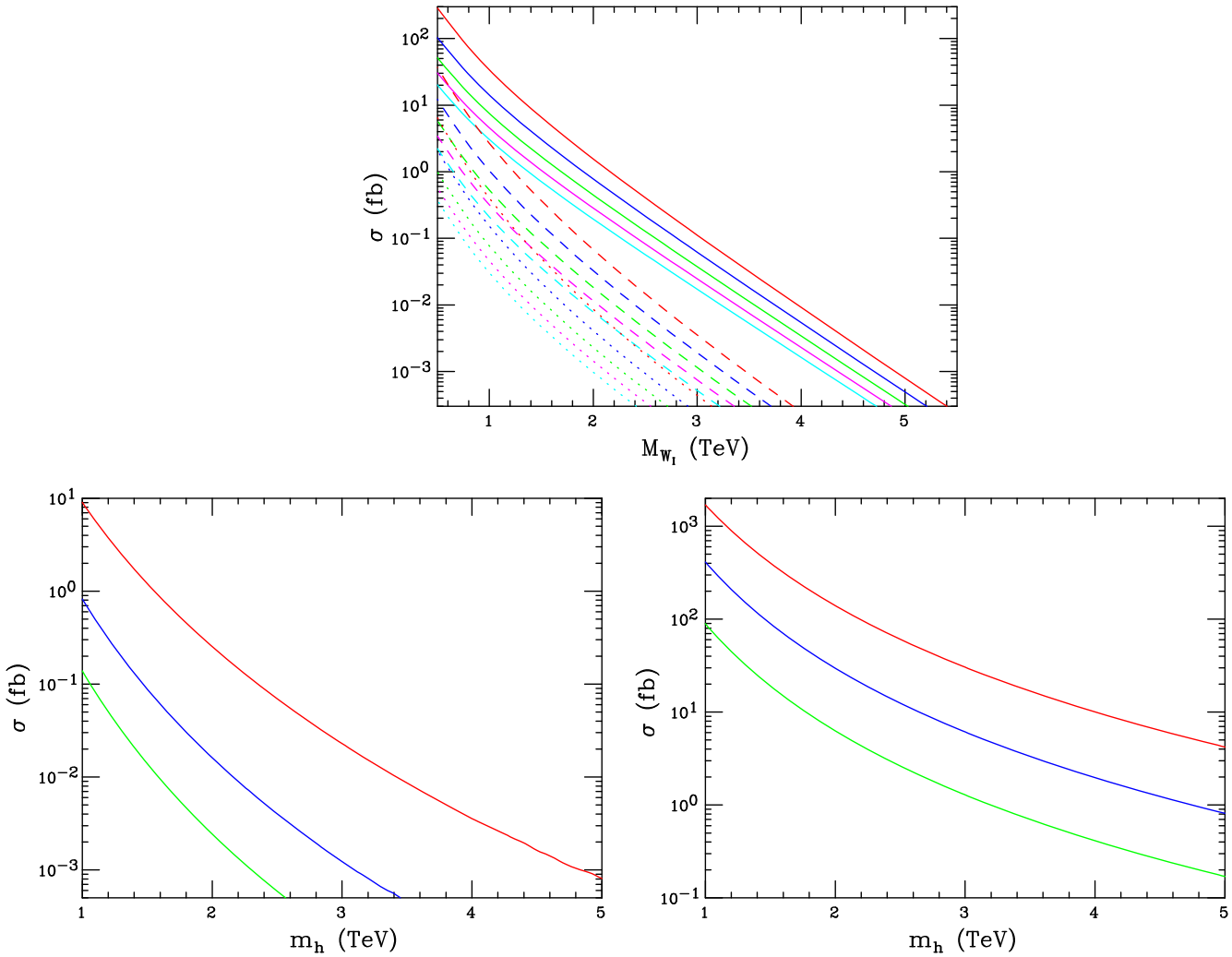

FIG. 13. (Top) The $W_I^{(\dagger)}A_I/S$ associated production cross section as a function of m_{W_I} and in units of $(g_I\lambda/g)^2$ at the $\sqrt{s} = 14$ TeV LHC. Here the curves are for the choice of $d\bar{d}$ (solid), $s\bar{s}$ (dashed) or $b\bar{b}$ (dotted) initial states assuming, from top to bottom in each set, that $m_h = 1, \ldots, 5$ TeV, respectively. (Bottom left) A_I or S pair production cross section in units of λ^4 as a function of m_h assuming, from top to bottom, $q = d$, s, b, respectively. (Bottom right) $A_I S$ associated production cross section in units of λ^4 as a function of m_h assuming, from top to bottom, $q = d$, s, b, respectively.

the set of Higgs fields that we have already introduced above, H_i, most of the neutral fermion states ν, N, $S_{1,2}$ will generally obtain Dirac masses and mix among themselves such that their gauge interactions will allow for their eventual decays down to SM particles and thus *none* of them can be the required stable DM. Interestingly, at the renormalizable level so far discussed, one linear combination of these states will necessarily remain massless (due to a lack of a partner with the opposite chirality) and may only obtain its mass via the introduction of Majorana mass terms or, more generally, via the introduction of higher-dimensional operators; these possibilities will warrant further study elsewhere. The only other SM neutral fields that we have seen above are the chiral doublet and triplet fields, D, T, for which we would need to produce Majorana mass terms and that were introduced simply to cancel the gauge/gravity anomalies. Such states are not likely to be present in a top-down approach or in the next step up the ladder to a more UV-complete theory where such cancellations are generally more subtle.

The implications of these considerations in the bottom-up approach are that we need to introduce a further new neutral, SM singlet state to play the role of DM without upsetting either the anomaly cancellation conditions or the requirements associated with the finiteness of the ϵ parameter. One tempting choice is to add to the fermion spectrum a new vector-like, SM singlet, S_3, with a mass M_3 (which we assume to be somewhat fine-tuned) that is of order $\sim O(1\ \text{GeV})$, but which is also an $SU(2)_I$ singlet and carries a dark charge $Q_D(S_3) = -Q_D(S_1) = 1 = Y_{I'}$ since such a state also has $T_{3I} = 0$. Given the set of Higgs fields H_i above, S_3 will not mix with any of the other neutral

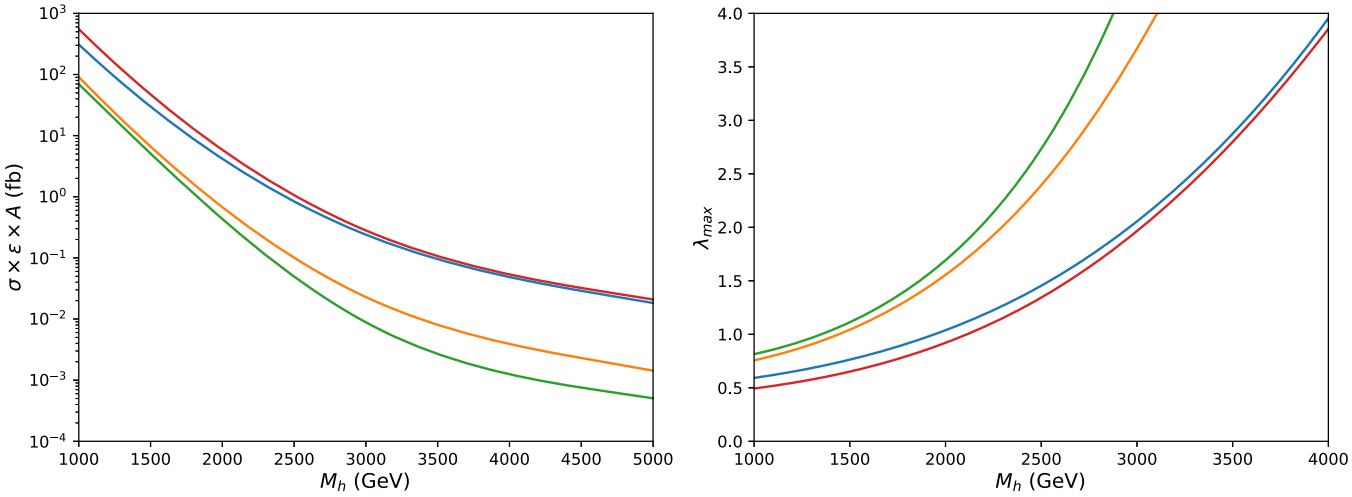

FIG. 14. (Left) The signal cross section $\sigma \times \epsilon \times A$ for IM1 for $pp \to 2A_I, 2S, A_I S + 1 - 4j$ as a function of m_h up to an overall factor of λ^4 at the $\sqrt{s} = 13$ TeV LHC in the 5FNS. IM1 corresponds to $E_T^{\rm miss} > 250$ GeV in addition to the cuts on jets and leptons described in the text. The red (blue, gold, green) line corresponds to h coupling to all generations (only d, only s, only b). As m_h increases, the case of universal couplings becomes increasingly dominated by the first generation. (Right) Upper bounds on λ from the monojet search of Ref. [49]. As m_h increases, the case of universal couplings is dominated by the first generation and the upper bounds on λ converge.

fields that we have already introduced (at the renormalizable level) and hence it will have no obvious decay paths allowing it to be stable. Such states can arise naturally, or at least in a less *ad hoc* fashion, at the next step towards a more UV-complete model [18].

The state S_3, by virtue of having a nonzero Q_I charge, will couple to the Z_I in addition to A_I. Since the Z_I is much more massive than the DM, with $m_{Z_I} \simeq 5$ TeV, it will be a subleading contribution to DM-electron scattering. At high temperatures in the early Universe, the Z_I interaction may help bring the DM into thermal equilibrium with the SM, and Z_I-mediated reactions will freeze out long before A_I-mediated reactions, so the latter will control the relic density. However, it is well known that scenarios with light Dirac fermion states with masses less than a few GeV are constrained by measurements of the cosmic microwave background (CMB) power spectrum [50]. These constraints arise from DM annihilating via s-wave processes into SM electromagnetic final states (e.g., e^+e^-) so that light S_3 states annihilating via dark photons are excluded [51,52], as the annihilation cross section is guaranteed to be s wave, either proceeding through s-channel A_I exchange for $m_{S_3} < m_{A_I}$ or through the t-channel process $S_3 S_3 \to A_I A_I$ for $m_{S_3} > m_{A_I}$.

One alternative to these vector-like fermionic DM states is that a (purely) dark Higgs plays the role of dark matter. In the simplest scenario a complex scalar ϕ with mass $m_\phi \sim O(1\ \text{GeV}) < m_{A_I}$, charged only under $U(1)_I$ so that its interaction with the SM is mediated only by A_I and Z_I, will have p-wave annihilations into SM electromagnetic final states, thus avoiding the stringent CMB constraints. We note that $m_\phi < m_{A_I}$ is required for the annihilation cross section to be p-wave suppressed, as the process $\phi\phi \to A_I A_I$ is s wave, and would dominate for $m_\phi > m_{A_I}$.

While several physical scalar states remain after the symmetry breaking, as described at the end of Sec. III B, none fit the requirements of a stable, light, complex scalar thermal relic with interactions primarily mediated by A_I. The three physical charged states obviously cannot be dark matter, and in the neutral sector we do not have the proper degrees of freedom to form a light $U(1)_D$ charged scalar which only interacts via the dark gauge bosons A_I and Z_I. Three of the four electrically neutral states which carry $U(1)_D$ charge in the gauge eigenbasis, $h^0_{1,4}$ and $a^0_{1,4}$, are likely eaten by the A_I and $W_I^{(\dagger)}$, so that the remaining physical neutral states only have a single real CP-even $U(1)_D$ charged component. Indeed, since it is likely that $W_I^{(\dagger)}$ eats a Goldstone which is predominantly h_4, the remaining state would likely have an appreciable interaction with the SM Z as well. In any event, this state cannot be combined with the presumably $U(1)_D$ neutral CP-odd field which remains after the symmetry breaking to form a complex scalar with $Q_D = 1$, so we see that the scalar DM described above must lie outside of the scalar field content proposed in Sec. III A to provide appropriate fermion masses.

One may well ask how the conventional DM physics associated with the canonical KM scenario, where DM-SM interactions are mediated by the exchange of a dark photon with purely vectorial couplings alone, is altered by the additional structure introduced above. In particular, we have in mind the calculation of the thermal relic cross section and the DM-electron scattering cross section, σ_e, as relevant for DM direct detection in this mass range $\sim$1 GeV. From the above discussions we know that this simple interaction picture is modified not only by the new

interactions introduced by the additional gauge bosons and their mixing with the corresponding SM fields but also by the mass mixing of the portal fields and the corresponding SM partners. While some of these effects will influence all of the SM fermions, other possible effects will, of course, be influenced by which SM generation mixes with the new exotic fields. It is interesting to note that the coupling of a single set of exotic fields to a specific SM generation would produce nonuniversal couplings which might be explored in flavor experiments, but a study of such effects is beyond the scope of this work. The case considered in Sec. III C dealt with a single exotic generation, but in principle there may be several exotic generations as was briefly discussed above. In this case there would be a rather more complex mass mixing structure, but the overall effect would remain roughly of the same order of magnitude. Certainly, if the single set of exotics couple only to the second or third generation, the influence of all the new portal matter fields on σ_e, will be completely absent at tree level. Fortunately, more generally, since both DM annihilation and electron scattering are dominated by the DM-DP $\sim$ GeV mass scales, or below, they are generally protected from much of this new physics, even when the exotics mix with the first SM generation, which is generally seen to decouple as is certainly the case with the new gauge interactions. For example, the influence of Z_I exchange is clearly inconsequential since its mass is likely (at least) several TeV, making a relative contribution to the amplitudes of both processes which is at most $\sim 10^{-3}$. The contributions of the W, W_I gauge bosons are similarly either mass mixing, mass ratio, or loop suppressed, or some combination of these. However, due to the $Z - A_I$ mixing discussed above, and the canonical kinetic mixing, all SM fields will experience a coupling to the DP given by the combination $e\epsilon Q - \sigma \frac{g}{c_w}(T_{3L} - s_w^2 Q)$ where $\sigma = (g g_I s_I)(v_1/m_Z)^2/(2c_w) \sim \epsilon$ as previously defined; note that σ can have either sign relative to ϵ. This $Z - A_I$ mixing term induced a parity-violating interaction between all the SM fermions and the DP. On top of this general effect, the mass mixing of, e.g., the first-generation SM fermions with the exotics can produce some additional nontrivial effects. As was discussed above and in **I**, $e - E$ mixing induces a new contribution to the A_I coupling which is purely left-handed and whose (relative) magnitude is controlled by the parameter ratio $y \simeq -e_I (v_4/v_3)^2/(e\epsilon)$, which may also have either sign. Thus for electrons, explicitly, one finds the DP coupling to be

$$e\epsilon \bar{e} \gamma_\mu (v_l - a_l \gamma_5) e A_I^\mu, \tag{46}$$

where $v_l = -1 - \frac{y}{2} - \frac{\sigma g}{2 c_w \epsilon e}(-\frac{1}{2} + 2 s_w^2)$ and $a_l = -\frac{y}{2} + \frac{\sigma g}{4 c_w \epsilon e}$, respectively. The first term in the vector coupling is the canonical one from KM, the second term arises from the $A_I - Z$ mass mixing induced by the light VEV of the bidoublet H_2, and the final term is induced by the $e - E$ mass mixing due to the light VEV of the $SU(2)_I$ doublet H_3. (This last term will, of course, be absent, i.e., $y \to 0$, if the exotics mix with the second- or third-generation SM fermions.) DM scattering off of electrons will then be modified by an overall factor of $v_l^2 + a_l^2$ relative to the canonical KM result. For a DM pair annihilating into $e^+ e^-$, since we are far above threshold there is also an identical rescaling factor. However, if the exotics mix with the second SM generation, near but above the $\mu^+ \mu^-$ threshold, the impact is a bit more complex with a rescaling of the canonical result for this final state by a factor of $v_l^2 + 2\beta^2 a_l^2/(3 - \beta^2)$, where to lowest order in the velocity expansion $\beta^2 = 1 - (m_\mu/m_{\rm DM})^2$. Once above the hadronic threshold, the existence of both v_l, $a_l \neq 0$ will reweight the usual annihilation cross sections in a complex manner as various specific particle thresholds are crossed but these effects will remain $O(1)$.

VI. DISCUSSION AND CONCLUSIONS

The dark photon as a mediator between the dark sector and the SM provides a compelling scenario for extending the WIMP idea to smaller DM masses. However, the generation of the necessary kinetic mixing at one loop requires the existence of new states—portal matter—which are charged under both the SM and the dark $U(1)_D$ gauge group. In order to satisfy anomaly freedom, constraints from precision Higgs/electroweak data as well as those on particle lifetimes from nucleosynthesis, these portal matter states must be vector-like (with respect to the SM gauge symmetries) copies of (at least some of) the SM fermions. Furthermore, if the strength of the kinetic mixing is a finite quantity, as might be expected in a UV framework, then the various couplings of the portal matter states must be in some way correlated with one another as might be expected within a non-Abelian group structure.

In this work we took a bottom-up approach to building a theory of the portal matter necessary for one-loop kinetic mixing, beginning with fermionic matter inspired by E_6, but we augmented the $SU(5) \times SU(2)_I$ subgroup of E_6 by an additional $U(1)_I$, which kinetically mixes with the SM hypercharge. This allowed us to avoid a scenario where the SM fermions are charged under the eventual $U(1)_D$ group, as they would be if we identified $U(1)_D$ as a subgroup of $SU(2)_I$. The $SU(2)_I \times U(1)_I$ breaks to $U(1)_D$ at a scale of several TeV, leading to the generation of masses for the gauge bosons Z_I and $W_I^{(\dagger)}$ as well as the exotic fermions at the TeV scale. This TeV scale symmetry breaking can be probed at the LHC, primarily through the production of Z_I, $W_I^{(\dagger)}$, or the down-like quark partner h, and the absence of such signals to date allows us to place some constraints on the strength of the dark coupling constants and s_I^2, the analog of the weak mixing angle associated with the $SU(2)_I \times U(1)_I \to U(1)_D$ breaking pattern. The exotic

and SM fermions are both charged under $U(1)_I$, so that both contribute to the kinetic mixing parameter ϵ. The relatively degenerate masses of the exotic fermions at the TeV scale and the SM fermions at the GeV scale allow the contributions to ϵ to be suppressed, so that the leading contributions go like $\log(\frac{m_E}{m_h})$ and $\log(\frac{m_e}{m_d})$. This cancellation generically gives $\epsilon \sim 10^{-(3-4)}$, an interesting portion of parameter space for dark matter.

The gauge charges of the exotic fermions impose requirements on the Higgs sector of the model, both to generate their TeV scale masses and to ensure mass mixings with SM fermions that allow them to decay promptly. Three scales emerge from the pattern of VEVs required to give the fermionic content of the theory appropriate masses while producing a GeV scale dark photon: the few-10-TeV-scale VEV v_3, responsible for the $SU(2)_I \times U(1)_I \to U(1)_D$ breaking and exotic fermion masses, the weak-scale VEVs v, v_2 responsible for the electroweak symmetry breaking of the SM and the SM fermion masses, and the GeV-scale VEVs v_1, v_4 which are responsible for breaking $U(1)_D$ as well as generating mass mixings which allow exotic fermion decay. Interestingly, since the light VEVs lie in the $SU(2)_I$ doublet and the $SU(2)_L \times SU(2)_I$ bidoublet, this symmetry breaking pattern creates a nonstandard phenomenology of the dark photon A_I, which now acquires a new coupling to the SM through mass mixing with the Z and a new SM-exotic coupling through mass mixing with the Hermitian combination $W_I + W_I^\dagger$. These mixing effects produce parity-violating couplings to the A_I in addition to the traditional vector $\epsilon e Q$ coupling. The additional Z-like coupling modifies cross sections in direct-detection experiments, and the SM-exotic coupling can produce a rich collider phenomenology, for instance allowing pair production of $h\bar{h}$ through t-channel A_I exchange, which was explored in Sec. IV. The mass mixing between exotic fermions and their SM counterparts can also induce new diagonal couplings to A_I, though these are subdominant and enter at order ϵ^2. For general SM-VLF mixings, FCNCs can yield some important constraints on the details of the model structure.

The extensive exotic field content of this model, and its original E_6 inspiration, beg the question of a top-down unified theory approach, which is the topic of a future work. The construction of such a model clearly requires a unifying group larger than E_6, and the vector-like dark fermionic states $S_{1,2,3}$ hint at a unification of $SU(2)_I \times U(1)_I \to SU(3)_I$ in a GUT context. Furthermore, the GUT symmetry-breaking pattern may yield a more predictive phenomenology by fixing the relative coupling strengths and mixing angles which were treated as free parameters above. This further work should also seek to provide a more compelling dark matter candidate, as there are quite tight constraints for DM coupling to a kinetically mixed dark photon in the GeV mass range.

In summary, we have analyzed the implications of fermionic portal matter inspired by the exotic content of $E_6/SU(2)_I$-based models, which gives rise to a kinetic mixing between a massive dark photon A_I and the SM photon. Requiring that the exotic fermions have TeV-scale masses and decay into SM particles implies a Higgs and gauge sector which has many nonstandard couplings as outlined in Sec. III, and a rich phenomenology which may be explored in low-energy experiments and at colliders as detailed in Sec. IV. The question of thermal dark matter and the implications of the nonstandard couplings of the dark photon for direct-detection experiments were summarized in Sec. V, and a further exploration of a unified theory approach is reserved for future work.

ACKNOWLEDGMENTS

T. G. R. would like to thank J. L. Hewett for discussions related to this work. This work was supported by the Department of Energy, Contract DE-AC02-76SF00515.

[1] M. Kawasaki and K. Nakayama, Annu. Rev. Nucl. Part. Sci. **63**, 69 (2013).
[2] P. W. Graham, I. G. Irastorza, S. K. Lamoreaux, A. Lindner, and K. A. van Bibber, Annu. Rev. Nucl. Part. Sci. **65**, 485 (2015).
[3] For a recent review of WIMPs, see G. Arcadi, M. Dutra, P. Ghosh, M. Lindner, Y. Mambrini, M. Pierre, S. Profumo, and F. S. Queiroz, Eur. Phys. J. C **78**, 203 (2018).
[4] J. Alexander *et al.*, arXiv:1608.08632.
[5] M. Battaglieri *et al.*, arXiv:1707.04591.
[6] N. Aghanim *et al.* (Planck Collaboration), arXiv:1807.06209.
[7] There has been a huge amount of work on this subject; see, for example, D. Feldman, B. Kors, and P. Nath, Phys. Rev. D **75**, 023503 (2007); D. Feldman, Z. Liu, and P. Nath, Phys. Rev. D **75**, 115001 (2007); M. Pospelov, A. Ritz, and M. B. Voloshin, Phys. Lett. B **662**, 53 (2008); M. Pospelov, Phys. Rev. D **80**, 095002 (2009); H. Davoudiasl, H. S. Lee, and W. J. Marciano, Phys. Rev. Lett. **109**, 031802 (2012); Phys. Rev. D **85**, 115019 (2012); R. Essig *et al.*, arXiv:1311.0029; E. Izaguirre, G. Krnjaic, P. Schuster, and N. Toro, Phys. Rev. Lett. **115**, 251301 (2015); M. Khlopov, Int. J. Mod. Phys. A **28**, 1330042 (2013); For a general overview and introduction to this

framework, see D. Curtin, R. Essig, S. Gori, and J. Shelton, J. High Energy Phys. 02 (2015) 157.
[8] B. Holdom, Phys. Lett. **166B**, 196 (1986); Phys. Lett. B **178**, 65 (1986); K. R. Dienes, C. F. Kolda, and J. March-Russell, Nucl. Phys. **B492**, 104 (1997); F. Del Aguila, Acta Phys. Pol. B **25**, 1317 (1994); K. S. Babu, C. F. Kolda, and J. March-Russell, Phys. Rev. D **54**, 4635 (1996); T. G. Rizzo, Phys. Rev. D **59**, 015020 (1998).
[9] T. G. Rizzo, Phys. Rev. D **99**, 115024 (2019).
[10] See, for example, the last two papers in Ref. [8].
[11] For a recent overview of vector-like quarks and original references, see C. Y. Chen, S. Dawson, and E. Furlan, Phys. Rev. D **96**, 015006 (2017); for a corresponding recent overview of vector-like leptons and original references, see Z. Poh and S. Raby, Phys. Rev. D **96**, 015032 (2017); For a general recent review of VLF, see V. Peralta, arXiv: 1712.06193.
[12] M. Aaboud *et al.* (ATLAS Collaboration), arXiv:1808 .02343; A. M. Sirunyan *et al.* (CMS Collaboration), arXiv:1805.04758; CMS Collaboration, CERN Report No. CMS-PAS-EXO-18-005, 2018.
[13] M. Tanabashi *et al.* (Particle Data Group), Phys. Rev. D **98**, 030001 (2018).
[14] See, however, some earlier general discussions in B. Patt and F. Wilczek, arXiv:hep-ph/0605188; H. Davoudiasl, R. Kitano, T. Li, and H. Murayama, Phys. Lett. B **609**, 117 (2005); D. McKeen, M. Pospelov, and A. Ritz, Phys. Rev. D **86**, 113004 (2012); B. Batell, M. Pospelov, A. Ritz, and Y. Shang, Phys. Rev. D **81**, 075004 (2010); J. H. Kim, S. D. Lane, H. S. Lee, I. M. Lewis, and M. Sullivan, arXiv: 1904.05893.
[15] For a review, see J. L. Hewett and T. G. Rizzo, Phys. Rep. **183**, 193 (1989).
[16] T. Gherghetta, J. Kersten, K. Olive, and M. Pospelov, Phys. Rev. D **100**, 095001 (2019).
[17] D. London and J. L. Rosner, Phys. Rev. D **34**, 1530 (1986).
[18] T. D. Rueter and T. G. Rizzo (to be published).
[19] For a classic review and original references, see R. N. Mohapatra, *Unification and Supersymmetry* (Springer, New York, 1986).
[20] G. C. Branco, P. M. Ferreira, L. Lavoura, M. N. Rebelo, M. Sher, and J. P. Silva, Phys. Rep. **516**, 1 (2012).
[21] M. S. Chanowitz and M. K. Gaillard, Nucl. Phys. **B261**, 379 (1985); B. W. Lee, C. Quigg, and H. B. Thacker, Phys. Rev. D **16**, 1519 (1977); J. M. Cornwall, D. N. Levin, and G. Tiktopoulos, Phys. Rev. D **10**, 1145 (1974); **11**, 972(E) (1975); G. J. Gounaris, R. Kogerler, and H. Neufeld, Phys. Rev. D **34**, 3257 (1986).
[22] P. D. Bolton, F. F. Deppisch, C. Hati, S. Patra, and U. Sarkar, Phys. Rev. D **100**, 035013 (2019).
[23] K. Ishiwata, Z. Ligeti, and M. B. Wise, J. High Energy Phys. 10 (2015) 027.
[24] C. Bobeth, A. J. Buras, A. Celis, and M. Jung, J. High Energy Phys. 04 (2017) 079.
[25] C. Bobeth, A. J. Buras, A. Celis, and M. Jung, J. High Energy Phys. 07 (2017) 124.
[26] H. Leutwyler and M. Roos, Z. Phys. C **25**, 91 (1984).
[27] P. Ball and R. Zwicky, Phys. Rev. D **71**, 014015 (2005).
[28] M. Tanabashi *et al.* (Particle Data Group), Phys. Rev. D **98**, 030001 (2018).
[29] *BABAR* Collaboration, Phys. Rev. D **87**, 112005 (2013).
[30] G. Aad *et al.* (ATLAS Collaboration), Phys. Lett. B **796**, 68 (2019).
[31] ATLAS Collaboration, Prospects for searches for heavy Z' and W' bosons in fermionic final states with the ATLAS experiment at the HL-LHC, CERN Report No. ATL-PHYS-PUB-2018-044, 2018.
[32] M. Aaboud *et al.* (ATLAS Collaboration), J. High Energy Phys. 01 (2018) 055.
[33] ATLAS Collaboration, Prospects for the search for additional Higgs bosons in the ditau final state with the ATLAS detector at HL-LHC, CERN Report No. ATL-PHYS-PUB-2018-050, 2018.
[34] We employ numerical estimates based on M. Czakon and A. Mitov, Comput. Phys. Commun. **185**, 2930 (2014); and also M. Aliev, H. Lacker, U. Langenfeld, S. Moch, P. Uwer, and M. Wiedermann, Comput. Phys. Commun. **182**, 1034 (2011).
[35] We use as a check of our numerical calculations the results of the LHC Top Physics Working Group, https://twiki.cern .ch/twiki/bin/view/LHCPhysics/LHCTopWG.
[36] N. Arkani-Hamed and N. Weiner, J. High Energy Phys. 12 (2008) 104; M. Baumgart, C. Cheung, J. T. Ruderman, L. T. Wang, and I. Yavin, J. High Energy Phys. 04 (2009) 014; A. Falkowski, J. T. Ruderman, T. Volansky, and J. Zupan, Phys. Rev. Lett. **105**, 241801 (2010); J. High Energy Phys. 05 (2010) 077; C. Cheung, J. T. Ruderman, L. T. Wang, and I. Yavin, J. High Energy Phys. 04 (2010) 116; G. Barello, S. Chang, C. A. Newby, and B. Ostdiek, Phys. Rev. D **95**, 055007 (2017).
[37] For some related LHC searches, see M. Aaboud *et al.* (ATLAS Collaboration), Phys. Rev. D **99**, 052005 (2019); A. M. Sirunyan *et al.* (CMS Collaboration), J. High Energy Phys. 02 (2019) 179; A. M. Sirunyan *et al.* (CMS Collaboration), Phys. Rev. D **99**, 032011 (2019).
[38] G. Aad *et al.* (ATLAS Collaboration), J. High Energy Phys. 11 (2014) 088; 02 (2016) 062; M. Del Gaudio (ATLAS Collaboration), Proc. Sci., EPS-HEP2017 (**2018**) 690; ATLAS note ATLAS-CONF-2016-042; V. Khachatryan *et al.* (CMS Collaboration), Phys. Lett. B **752**, 146 (2016); CMS Collaboration, CERN Report No. CMS-PAS-HIG-18-003, 2018.
[39] C. Alpigiani *et al.*, A letter of intent for MATHUSLA: A dedicated displaced vertex detector above ATLAS or CMS, CERN Report No. CERN-LHCC-2018-025, LHCC-I-031, 2018.
[40] A. Ariga *et al.* (FASER Collaboration), arXiv:1811.10243.
[41] S. S. D. Willenbrock and D. A. Dicus, Phys. Lett. **156B**, 429 (1985).
[42] P. N. Bhattiprolu and S. P. Martin, Phys. Rev. D **100**, 015033 (2019).
[43] Cross sections can be easily obtainable with small modifications to the results as presented in J. F. Gunion, J. L. Hewett, E. Ma, T. G. Rizzo, V. D. Barger, N. Deshpande, and K. Whisnant, Int. J. Mod. Phys. A **02**, 1199 (1987).
[44] Y. do Amaral Coutinho, J. A. Martins Simoes, and M. C. Pommot Maia, Phys. Rev. D **45**, 771 (1992).
[45] A. Alloul, N. D. Christensen, C. Degrande, C. Duhr, and B. Fuks, Comput. Phys. Commun. **185**, 2250 (2014).

[46] J. Alwall, R. Frederix, S. Frixione, V. Hirschi, F. Maltoni, O. Mattelaer, H. S. Shao, T. Stelzer, P. Torrielli, and M. Zaro, J. High Energy Phys. 07 (2014) 079.
[47] T. Sjöstrand, S. Ask, J. R. Christiansen, R. Corke, N. Desai, P. Ilten, S. Mrenna, S. Prestel, C. O. Rasmussen, and P. Z. Skands, Comput. Phys. Commun. **191**, 159 (2015).
[48] J. De Favereau, C. Delaere, P. Demin, A. Giammanco, V. Lemaitre, A. Mertens, and M. Selvaggi (Delphes 3 Collaboration), J. High Energy Phys. 02 (2014) 057.
[49] M. Aaboud *et al.* (ATLAS Collaboration), J. High Energy Phys. 01 (2018) 126.
[50] N. Aghanim *et al.* (Planck Collaboration), arXiv:1807.06209.
[51] M. S. Madhavacheril, N. Sehgal, and T. R. Slatyer, Phys. Rev. D **89**, 103508 (2014).
[52] H. Liu, T. R. Slatyer, and J. Zavala, Phys. Rev. D **94**, 063507 (2016).